

Supporting Information for:

New Powerful and Oxidatively Rugged Dinuclear Ru Water Oxidation Catalyst: Control of Mechanistic Pathways by Tailored Ligand Design

Sven Neudeck,[†] Somnath Maji,[‡] Isidoro López,[‡] Steffen Meyer,[†] Franc Meyer^{†*} and Antoni Llobet^{‡#}

[†] Institute of Inorganic Chemistry, Georg-August-University Göttingen, Tammannstr. 4, D-37077 Göttingen (Germany)

[‡] Institute of Chemical Research of Catalonia (ICIQ), Av. Països Catalans 16, E-43007 Tarragona (Spain)

[#] Departament de Química, Universitat Autònoma de Barcelona, 08460 Cerdanyola del Vallès, Barcelona (Spain)

Content

Experimental Section.....	2
Synthesis of {Na ₃ [1 (OH) ₂]·7.5H ₂ O}	4
Synthesis of 2(PF ₆) ₂	5
NMR Spectroscopy.....	6
Electrochemistry.....	16
Spectrophotometric Redox Titration.....	21
Catalysis Experiments	24
Exchange Kinetics	25
Labeling Experiments.....	29
Species after Catalysis.....	33
X-Ray Crystallography	34
References	35

Experimental Section

Materials

$\text{RuCl}_2(\text{dmsO})_4$ ^[1] and 3,5-Bis{6-(2,2'-bipyridyl)}-4-methyl-1*H*-pyrazole (H-Mebbp)^[2] were prepared according to literature procedures. High purity deionized water was obtained by passing it through an UltraClear water purifier system (SG Wasseraufbereitung und Regeneration GmbH) or by using an Aquatron A4000D automatic water still (Bibby Scientific). Trifluoromethanesulfonic acid (99+%), triflic acid, packed in ampules, was purchased from STREAM/CYMIT and ceric ammonium nitrate (Ce(IV), CAN) was used either from ABCR (99% ACS grade, for catalysis experiments) or from Aldrich ($\geq 99.99\%$ trace metal basis, for stoichiometric uses).

All other reagents were purchased from Aldrich Chemical Co. or ABCR and used without further purification. The utilized solvents were Chromasolve HPLC grade. All reactions were routinely performed under a nitrogen atmosphere by using standard *Schlenk* techniques.

NMR Spectroscopy

NMR Spectra were recorded on Avance DRX 500 (Bruker), Avance 500 Ultrashield (Bruker), Avance 300 (Bruker) and Avance III 300 (Bruker) instruments in D_2O , DOTf in D_2O ($c = 0.1 \text{ mol}\cdot\text{L}^{-1}$) or acetone- d_6 with residual protons as internal references.

Elemental analysis

Elemental analyses were performed in the Analytical Laboratory of the Institute of Inorganic Chemistry at the University of Göttingen using an Elementar 4.1 Vario EL 3 instrument.

Electrochemistry

Cyclic Voltammetry (CV) and Square Wave Voltammetry (SWV) experiments were performed either on a Model 263A (PerkinElmer) or a CHI-660 (IJ-Cambria scientific) potentiostat. Glassy carbon disk electrodes (2 mm) were used as working, platinum wire as auxiliary and a SCE as reference electrode. Glassy carbon disk electrodes were polished with $0.05 \mu\text{m}$ alumina paste and all electrodes were washed with water and acetone and air dried before use. Complexes were dissolved in propylene carbonate containing tetrabutylammoniumhexafluorophosphate ($[\text{N}^+\text{Bu}_4]\text{PF}_6$, $c = 0.1 \text{ mol}\cdot\text{L}^{-1}$) as electrolyte or aqueous trifluoromethanesulfonic acid solution ($c = 0.1 \text{ M}$, pH 1).

For construction of the Pourbaix Diagram a solution of complex $\{\mathbf{1}(\text{H}_2\text{O})_2\}^+$ ($c = 1\cdot 10^{-3} \text{ mol}\cdot\text{L}^{-1}$) in aqueous triflic acid ($c = 1.0 \text{ mol}\cdot\text{L}^{-1}$, pH 0) was used ($I = 1 \text{ M}$). Small amounts of aqueous sodium hydroxide solution (approximately $c = 10 \text{ mol}\cdot\text{L}^{-1}$) were added and the pH values were measured with a 780M pH meter (Metrohm) using an Ecotrode Plus (Metrohm) pH electrode. For each pH value a set of different CV and SWV experiments were carried out using the following parameter. CV: Scan rate = 100 mVs^{-1} , SWV: Scan rate = 20 mVs^{-1} , Pulse Height = 33 mV, Pulse Width = 100 ms, Step Height = 4 mV. Between each measurement the solution was stirred to renew the double layer and before going to the next pH value as well as between the CV and the SWV experiments the glassy carbon disk electrode was polished with $0.05 \mu\text{m}$ alumina paste and all electrodes were washed with water and acetone and air dried.

$E_{1/2}$ values for the Pourbaix diagram were obtained from SWV measurements. In order to distinguish overlapping signals, experimental data close to the peak maxima were treated with Lorentzian curves using the program *Fityk*^[3]. In the case of the fourth oxidation (1.15 V at pH 0) the thermodynamic potential could not be derived from CV or SWV measurements and thus the potential of the oxidative wave in CV is reported instead. The oxidation at 1.5 V is assigned to an over oxidation of the intermediate species after water nucleophilic attack. Theoretical values for simple electron transfer processes (0 mV per pH unit), $1 \text{ H}^+/1\text{e}^-$ -processes (59 mV per pH unit) and $2 \text{ H}^+/1\text{e}^-$ -processes (118 mV per pH unit) are indicated by solid lines (see Figure 2 main article).

Spectrophotometric redox titrations

Spectrophotometric redox titrations were performed on a Cary 50 Bio (Varian) instrument by sequential addition of 5 μL of a solution of ceric ammonium nitrate ($c = 1.29\cdot 10^{-3} \text{ mol}\cdot\text{L}^{-1}$) in aqueous triflic acid ($c = 0.1 \text{ mol}\cdot\text{L}^{-1}$, pH 1) to 3 mL of a solution of the complex ($2.40\cdot 10^{-5} \text{ mol}\cdot\text{L}^{-1}$) in aqueous triflic acid ($c = 0.1 \text{ mol}\cdot\text{L}^{-1}$, pH 1). Each addition corresponds to 0.09 equivalents of oxidant.

Exchange Kinetics

The exchange kinetics were monitored on a Cary 50 Bio (Varian) instrument (in the case of oxidation state II,II) and on a Specord S 100 (Analytik Jena) diode array spectrophotometer (in the case of higher oxidation states) equipped with a sample changer in 1 cm quartz cuvettes at 25.0°C (in the case of oxidation state II,II) and 27.6°C (in the case of higher oxidation states) at three different complex concentrations in the range of $c = 1.68\cdot 10^{-5} \text{ mol}\cdot\text{L}^{-1}$ to $3.58\cdot 10^{-5} \text{ mol}\cdot\text{L}^{-1}$.

In a typical experiment 10 μL acetonitrile (corresponding to a 2000 to 6000 fold excess) were added to 1.8 (in the case of oxidation state II,II) or 2.5 mL (in the case of higher oxidation states) of a complex solution in aqueous triflic acid ($c = 0.1 \text{ mol}\cdot\text{L}^{-1}$, pH 1), mixed and the UV-vis spectra recorded as fast as possible. To achieve higher oxidation states one or two equivalents of Ce(IV) solution (25 or 50 μL) in aqueous triflic acid ($c = 0.1 \text{ mol}\cdot\text{L}^{-1}$, pH 1) were added before the addition of MeCN. SPECFIT/32 (Version 3.0) was used to process data and to obtain rate constants by using models for mono or disubstitution reactions.

Decay Kinetics

The stability of all oxidation states was monitored on a Specord S 100 (Analytik Jena) diode array spectrophotometer equipped with a sample changer in 1 cm quartz cuvettes at 27.6 °C at different complex concentrations in the range of $c = 2.62 \cdot 10^{-5} \text{ mol} \cdot \text{L}^{-1}$ to $3.58 \cdot 10^{-5} \text{ mol} \cdot \text{L}^{-1}$. In a typical experiment the UV-vis spectra of 2.5 mL of a complex solution in aqueous triflic acid ($0.1 \text{ mol} \cdot \text{L}^{-1}$, pH 1) were monitored as fast as possible. SPECFIT/32 (Version 3.0) was used to process data and to obtain rate constants for the decay by using a simple one step reaction model.

Catalysis Experiments

Catalysis experiments were performed in a homemade thermostated glass cell ($V = 16.5 \text{ mL}$) at 25.0 °C which was closed with a septum. The evolution of gases were monitored by on-line manometry with a differential pressure manometer (Testo 521-1) which was connected to a reference cell of approximately the same size, as well as by a gas phase oxygen sensor (Ox-N sensor and Oxy-meter, Unisense) which was purged through the septum. The oxygen sensor was calibrated before each experiment by addition of known amounts of oxygen to the cell equipped with 2 mL of degassed aqueous triflic acid ($c = 0.1 \text{ mol} \cdot \text{L}^{-1}$, pH 1).

In a typical experiment the measurement cell with the complex was degassed and 1.85 mL of degassed aqueous triflic acid ($c = 0.1 \text{ mol} \cdot \text{L}^{-1}$, pH 1) were added with a Hamilton syringe. After pressure equilibration between reference and measurement cell, 150 μL of a degassed aqueous triflic acid ($c = 0.1 \text{ mol} \cdot \text{L}^{-1}$, pH 1) were added to the reference cell as soon as oxygen value and manometry signal were stable. 150 μL of a degassed solution of Ce(IV) in aqueous triflic acid ($c = 0.1 \text{ mol} \cdot \text{L}^{-1}$, pH 1) were added to the measurement cell resulting in a final concentration of the complex of $c = 1.0 \cdot 10^{-3} \text{ mol} \cdot \text{L}^{-1}$. Experiments with 1000 equivalents of Ce(IV) were performed by using diluted degassed solutions of the complex in the same setup and a final concentration of the complex of $c = 1.0 \cdot 10^{-4} \text{ mol} \cdot \text{L}^{-1}$.

TOF_i values were calculated from the manometry experiments with 100 equivalents of Ce(IV) by applying a linear fitting through the increase of TONs in the initial 30 s after addition of Ce(IV).

Labeling Experiments

Labelling experiments were performed by monitoring the evolution of different dioxygen isotopes within the first catalytic cycle by online mass spectrometry using an Omnistar GSD301 C (Pfeiffer) quadrupole mass spectrometer. Vials and solvents were degassed before use and all solutions were aqueous triflic acid solutions ($c = 0.1 \text{ mol} \cdot \text{L}^{-1}$, pH 1) using either deionized water (H_2^{16}O with natural abundance^[4] of 0.205 % ^{18}O , MilliQ quality) or H_2^{18}O (97 % ^{18}O , Cambridge Isotope Laboratories).

A typical experiment is described for the experiment in Table 2 (main article): A 3.6 μmol sample of complex was dissolved in 1.5 mL aqueous triflic acid (H_2^{16}O) and connected to the MS instrument. When a stable baseline was obtained, 2 equivalents of Ce(IV) dissolved in 250 μL aqueous triflic acid (H_2^{16}O) were added. As soon as all oxygen traces were stable 4 equivalents of Ce(IV) dissolved in 250 μL aqueous triflic acid (H_2^{18}O) were added. This produced a final solution with 0.20 % ^{18}O labeled catalyst and 12.3 % H_2^{18}O . The experiment was repeated with different ratios of ^{18}O at the catalyst and in the solution.

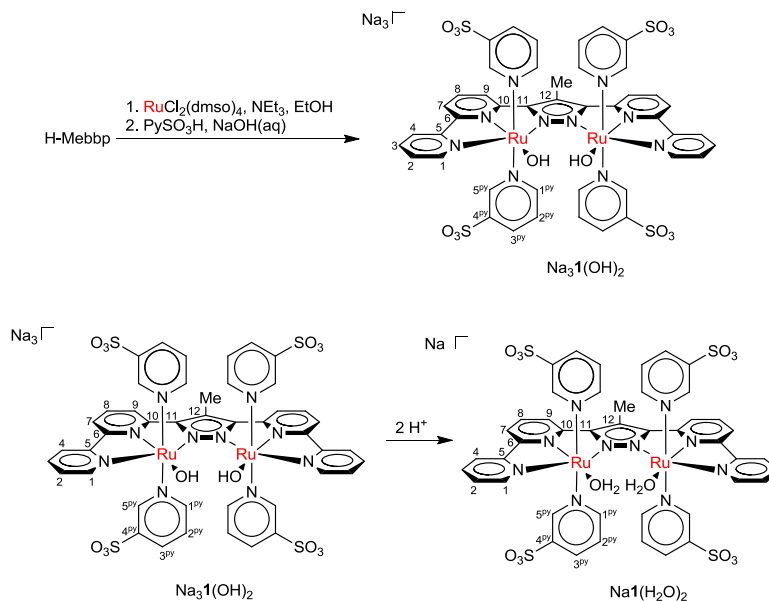
A linear background correction was applied to the dioxygen traces to balance the suction of the MS instrument. Therefore a linear fitting was applied to each trace at the end of the dioxygen evolution and the corresponding intensities were added. Time and intensity at the moment of Ce(IV) injection were set to zero. Values given in Table 2 (main article) and Table S2 (SI) were calculated from the final intensities.

X-Ray Crystallography

X-ray data were collected on a STOE IPDS II diffractometer with an area detector (graphite monochromated Mo-K α radiation, $\lambda = 0.71073 \text{ \AA}$) by use of ω scans at 133 K (Table S3). The structures were solved by direct methods (SHELXS-97) and refined on F² using all reflections with SHELXL-97.^[5] Non-hydrogen atoms were refined anisotropically. Hydrogen atoms were placed in calculated positions and assigned to an isotropic displacement parameter of 1.2 / 1.5 U_{eq}(C). Face-indexed absorption corrections were performed numerically with the program X-RED (X-RED; STOE & CIE GmbH, Darmstadt, Germany, 2002). In complex **2**(PF₆)₂, one PF₆⁻ counter anion was found to be disordered about a twofold rotation axis and was therefore refined with a fixed occupancy of 0.5. SADI restraints (d_{p-f} , d_{f-f}) and EADP constraints were applied to model the disorder.

CCDC-961171 contains the supplementary crystallographic data for **2**(PF₆)₂. These data can be obtained free of charge from The Cambridge Crystallographic Data Centre via http://www.ccdc.cam.ac.uk/data_request/cif.

Synthesis of {Na₃[1(OH)₂]-7.5H₂O}



A solution of H-Mebbp (154 mg, 0.39 mmol) and NEt₃ (1.0 mL, 7.2 mmol) in EtOH (45 mL) was slowly added under nitrogen atmosphere and refluxing conditions to a solution of RuCl₂(dmsO)₄ (444 mg, 0.92 mmol) in EtOH (10 mL). After additional reflux for two hours the solution was cooled to room temperature and a red precipitate was filtered off and washed with diethyl ether. The precipitate (150 mg) and 3-pyridinesulfonic acid (218 mg, 1.37 mmol) were suspended in aqueous NaOH (1.5 M, 2 mL) and refluxed overnight. The reaction mixture was cooled to 7 °C and the resulting brown precipitate was collected and washed with aqueous NaOH ($c = 1.5 \text{ mol} \cdot \text{L}^{-1}$). Recrystallization under nitrogen atmosphere from degassed aqueous NaOH ($c = 0.05 \text{ mol} \cdot \text{L}^{-1}$) by addition of degassed acetone afforded a brown precipitate which was filtered off, washed with acetone and diethyl ether and dried.

Yield: 126 mg, 0.0862 mmol, 22%

EA: Calc. (%): C: 36.14, H: 3.45, N: 9.58; S: 8.77 (for {Na₃[1(OH)₂]-7.5H₂O}: C₄₄H₅₀N₁₀Na₃O_{21.5}Ru₂S₄)

Found (%): C: 35.97, H: 3.21, N: 9.40, S: 8.99.

¹H-NMR (D₂O, 500 MHz): δ [ppm] = 9.01 (d, $J = 5.4$ Hz, 2H, 1-H), 8.13 – 8.02 (m, 12H, 4-H, 9-H, 1^{Py}-H, 5^{Py}-H), 7.88 (d, $J = 8.0$ Hz, 2H, 7-H), 7.84 – 7.79 (m, 2H, 3-H), 7.75 – 7.64 (m, 8H, 2-H, 8-H, 3^{Py}-H), 6.70 (dd, $J = 7.9, 5.9$ Hz, 4H, 2^{Py}-H), 2.97 (s, 3H, Me).

¹³C-NMR (D₂O, 75 MHz): δ [ppm] = 159.78 (2C, 6-C), 159.40 (2C, 5-C), 157.98 (2C, 10-C), 154.75 (4C, 1^{Py}-C), 150.71 (2C, 1-C), 150.26 (2C, 11-C), 148.25 (4C, 5^{Py}-C), 139.71 (4C, 4^{Py}-C), 136.83 (2C, 3-C), 133.33 (2C, 8-C), 133.06 (4C, 3^{Py}-C), 127.96 (2C, 2-C), 124.37 (4C, 2^{Py}-C), 122.97 (2C, 4-C), 121.64 (1C, 12-C), 119.66 (2C, 9-C), 118.52 (2C, 7-C), 9.73 (Me).

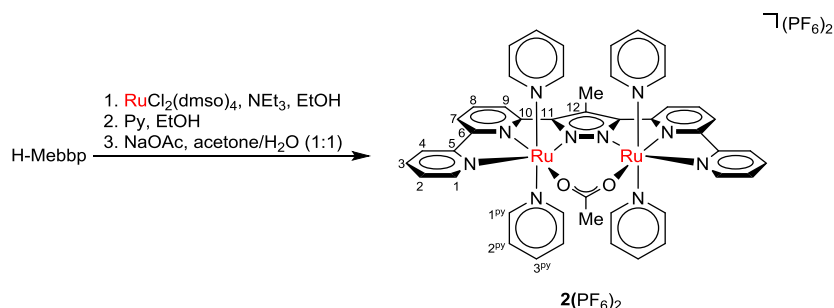
UV-vis ($c = 0.1 \text{ mol} \cdot \text{L}^{-1}$ aqueous triflic acid, pH 1) λ [nm] (ϵ [Lmol⁻¹cm⁻¹]): 250 ($3.1 \cdot 10^4$), 312 ($2.8 \cdot 10^4$), 360 ($2.7 \cdot 10^4$), 494 (sh, $4.3 \cdot 10^3$)

IR (KBr) $\tilde{\nu}$ [cm⁻¹]: 3081 (w), 1637 (m), 1595 (m), 1541 (w), 1506 (m), 1453 (s), 1387 (w), 1355 (w), 1213 (s), 1148 (s), 1062 (m), 1026 (s), 881 (w), 813 (m), 779 (m), 762 (m), 695 (m), 624 (s), 585 (m).

ESI-MS (MeOH/H₂O 1:1) m/z : pos: 1270.9 [1 - 2xH₂O + 2xNa]⁺, 1089.9 [1 - 2xH₂O - pySO₃ + Na]⁺, 908.9 [1 - 2xH₂O - 2xpySO₃]⁺, 647.0 [1 - 2xH₂O + 3 Na]²⁺; neg: 1083.9 [1 - 2xH₃O - pySO₃]⁻, 1065.9 [1 - 2xH₂O - pySO₃ - H]⁻, 630.0 [1 - H]²⁻, 621.0 [1 - H₃O]²⁻.

EChem: $E_{1/2}$ ($c = 1.0 \cdot 10^{-3} \text{ mol} \cdot \text{L}^{-1}$ in $0.1 \text{ mol} \cdot \text{L}^{-1}$ aqueous triflic acid, pH 1) [V vs. SCE]: 0.559, 0.857, 0.929, 1.056, 1.376, 1.506 (see Figure 2 and Table 1 of the main for assignment)

Synthesis of $2(\text{PF}_6)_2$



A solution of H-Mebbp (166 mg, 0.43 mmol) and NEt_3 (1.00 mL, 7.21 mmol) in EtOH (120 mL) was slowly added over 4 h under nitrogen atmosphere and refluxing conditions to a solution of $\text{RuCl}_2(\text{dmsO})_4$ (501 mg, 1.03 mmol) in EtOH (60 mL). Pyridine (6.00 mL, 74.4 mmol) was added and the mixture was heated at reflux for additional 6 h. The reaction mixture was cooled to room temperature, concentrated and aqueous NH_4PF_6 solution was added. The resulting precipitate was collected, washed with water and methyl *tert*-butyl ether and purified by column chromatography (neutral alumina, eluent: acetone/methanol 8:1). The red solid (150 mg) and NaOAc (214 mg, 2.62 mmol) were dissolved in a mixture of acetone and water (*v/v* 3:1, 40 mL) and the mixture was heated to reflux for 5 h. After cooling down to room temperature the mixture was concentrated until the formation of a red precipitate was observed. The precipitate was filtered off, washed with water and *tert*-butyl ether and dried. Crystals suitable for X-ray diffraction analysis were grown by slow diffusion of diethyl ether into a solution of $2(\text{PF}_6)_2$ in acetone.

Yield: 106 mg, 0.084 mmol, 20%

EA: Calc. (%): C: 43.92; H: 3.29; N: 11.13. (for $2(\text{PF}_6)_2$: $\text{C}_{46}\text{H}_{41}\text{F}_{12}\text{N}_{10}\text{O}_2\text{P}_2\text{Ru}_2$)

Found (%): C: 43.29; H: 3.24; N: 10.73.

$^1\text{H-NMR}$ (Acetone- d_6 , 300 MHz): δ [ppm] = 9.45 (ddd, J = 5.4, 1.5, 0.7 Hz, 2H, 1-H), 8.37 – 8.30 (m, 4H, 4-H, 9-H), 8.15 (dd, J = 8.0, 0.9 Hz, 2H, 7-H), 8.01 (td, J = 7.8, 1.6 Hz, 2H, 3-H), 7.92 – 7.85 (m, 4H, 2-H, 8-H), 7.80 (dt, J = 5.5, 1.5 Hz, 8H, 1^{py} -H), 7.39 (tt, J = 7.6, 1.5 Hz, 4H, 3^{py} -H), 6.80 – 6.74 (m, 8H, 2^{py} -H), 3.29 (s, 3H, Me), 3.03 (s, 3H, OAc).

$^{13}\text{C-NMR}$ (Acetone- d_6 , 75.5 MHz): δ [ppm] = 186.20 (1C, COO), 161.98 (2C, 6-C), 160.15 (2C, 5-C), 159.71 (2C, 10-C), 152.39 (8C, 1^{py} -C), 151.11 (2C, 1-C), 150.11 (2C, 11-C), 137.86 (2C, 3-C), 137.24 (4C, 3^{py} -H), 134.08 (2C, 8-C), 129.09 (2C, 2-C), 125.55 (8C, 2^{py} -H), 123.84 (2C, 4-C), 122.95 (1C, 12-C), 120.08 (2C, 9-C), 119.08 (2C, 7-C), 29.51 (1C, MeCOO), 10.70 (1C, Me).

UV-vis (MeNO $_2$, 0.1 M [N^tBu_4] PF_6) λ [nm]: 535, 611(sh), 681 (sh).

IR (KBr) $\tilde{\nu}$ [cm^{-1}]: 3011 (w), 3086 (w), 2923 (w), 2872 (w), 1593 (m), 1549 (m), 1487 (m), 1449 (m), 1410 (m), 1385 (w), 1352 (w), 1218 (w), 1032 (w), 841 (s), 767 (m), 698 (m), 558 (m).

ESI-MS (MeOH) m/z [%]: 1113.0 [$2 + \text{PF}_6$] $^+$, 484.0 [2] $^{2+}$, 421.0 [$2 - 2 \times \text{py} + \text{MeOH}$] $^{2+}$, 405.0 [$2 - 2 \times \text{py}$] $^{2+}$, 381.5 [$2 - 3 \times \text{py} + \text{MeOH}$] $^{2+}$, 342.0 [$2 - 4 \times \text{py} + \text{MeOH}$] $^{2+}$, 325.0 [$2 - 4 \times \text{py}$] $^{2+}$.

EChem: $E_{1/2}$ ($c = 1.0 \times 10^{-3} \text{ mol} \cdot \text{L}^{-1}$ in propylene carbonate, 0.1 $\text{mol} \cdot \text{L}^{-1}$ [N^tBu_4] PF_6) [V vs. SCE]: 0.64 ($\text{Ru}^{\text{III}}\text{Ru}^{\text{II}}/\text{Ru}^{\text{II}}\text{Ru}^{\text{II}}$), 1.04 ($\text{Ru}^{\text{III}}\text{Ru}^{\text{III}}/\text{Ru}^{\text{III}}\text{Ru}^{\text{II}}$)

NMR Spectroscopy

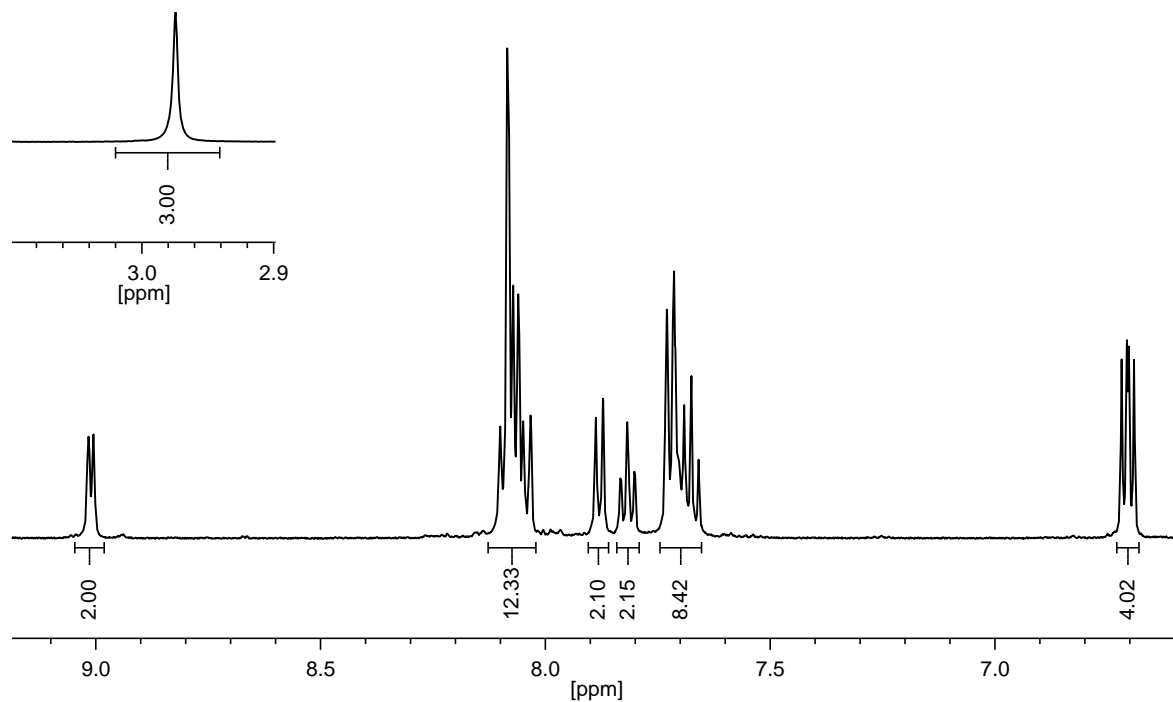


Figure S1: $^1\text{H-NMR}$ spectrum (500 MHz) of $\text{Na}_3\{1(\text{OH})_2\}$ in D_2O at 299 K.

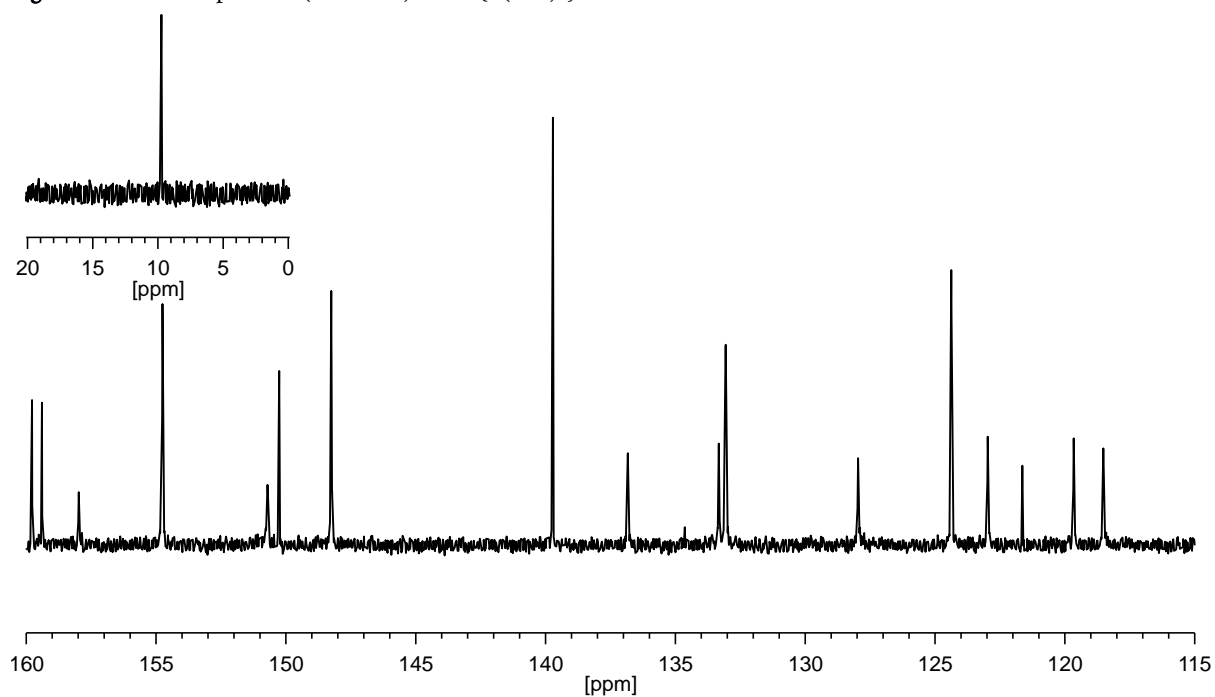


Figure S2: $^{13}\text{C-NMR}$ spectrum (75 MHz) of $\text{Na}_3\{1(\text{OH})_2\}$ in D_2O at 299 K.

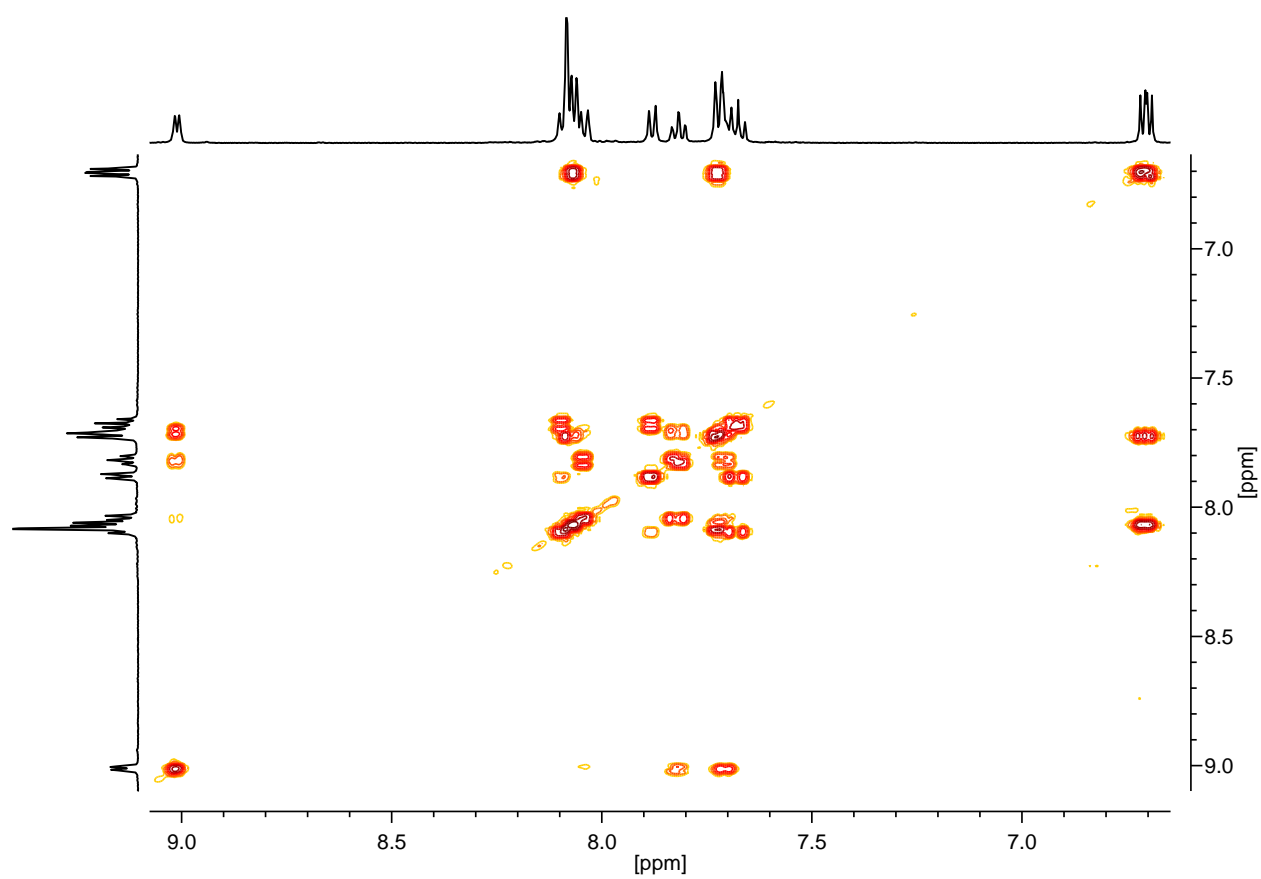


Figure S3: ^1H - ^1H -COSY spectrum of $\text{Na}_3\{\mathbf{1}(\text{OH})_2\}$ in D_2O at 299 K.

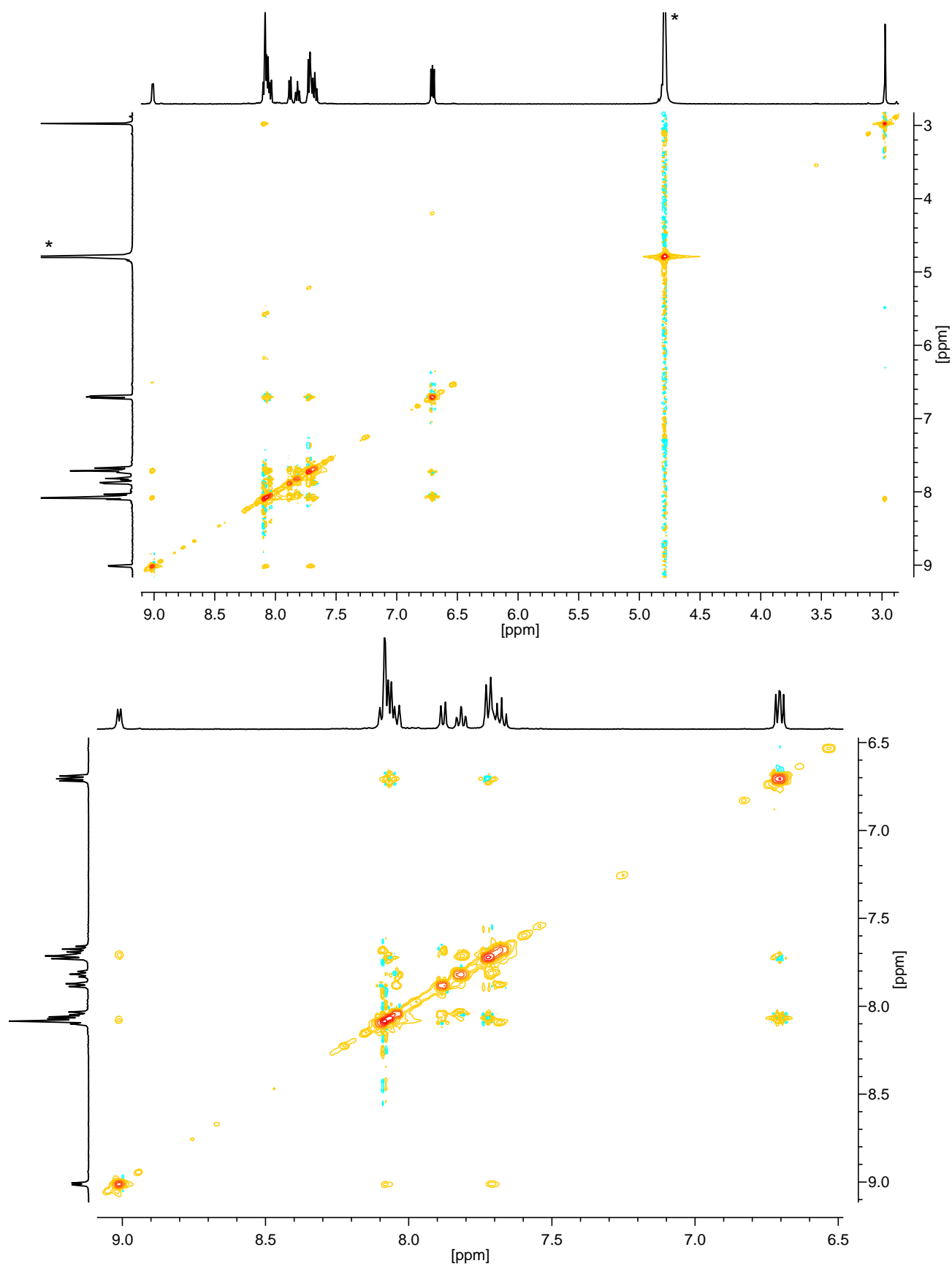


Figure S4: ^1H - ^1H -NOESY spectrum of $\text{Na}_3\{\mathbf{1}(\text{OH})_2\}$ in D_2O at 299 K (* H_2O). The lower part shows an expansion of the 6.5 – 9.1 ppm region.

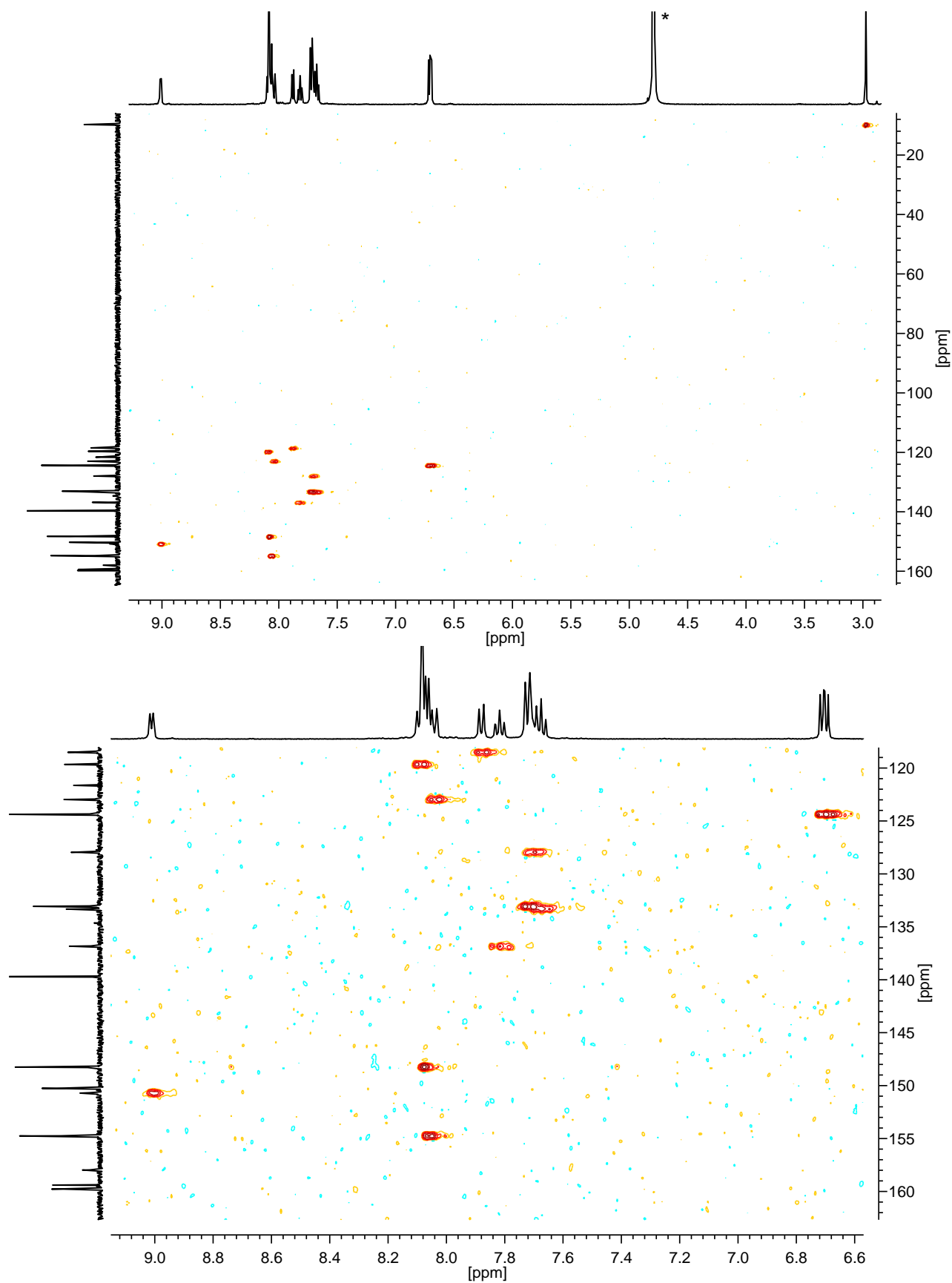


Figure S5: ^1H - ^{13}C -HSQC spectrum of $\text{Na}_3\{1(\text{OH})_2\}$ in D_2O at 299 K (* H_2O). The lower part shows an expansion of the 6.6 – 9.2 ppm region (^1H).

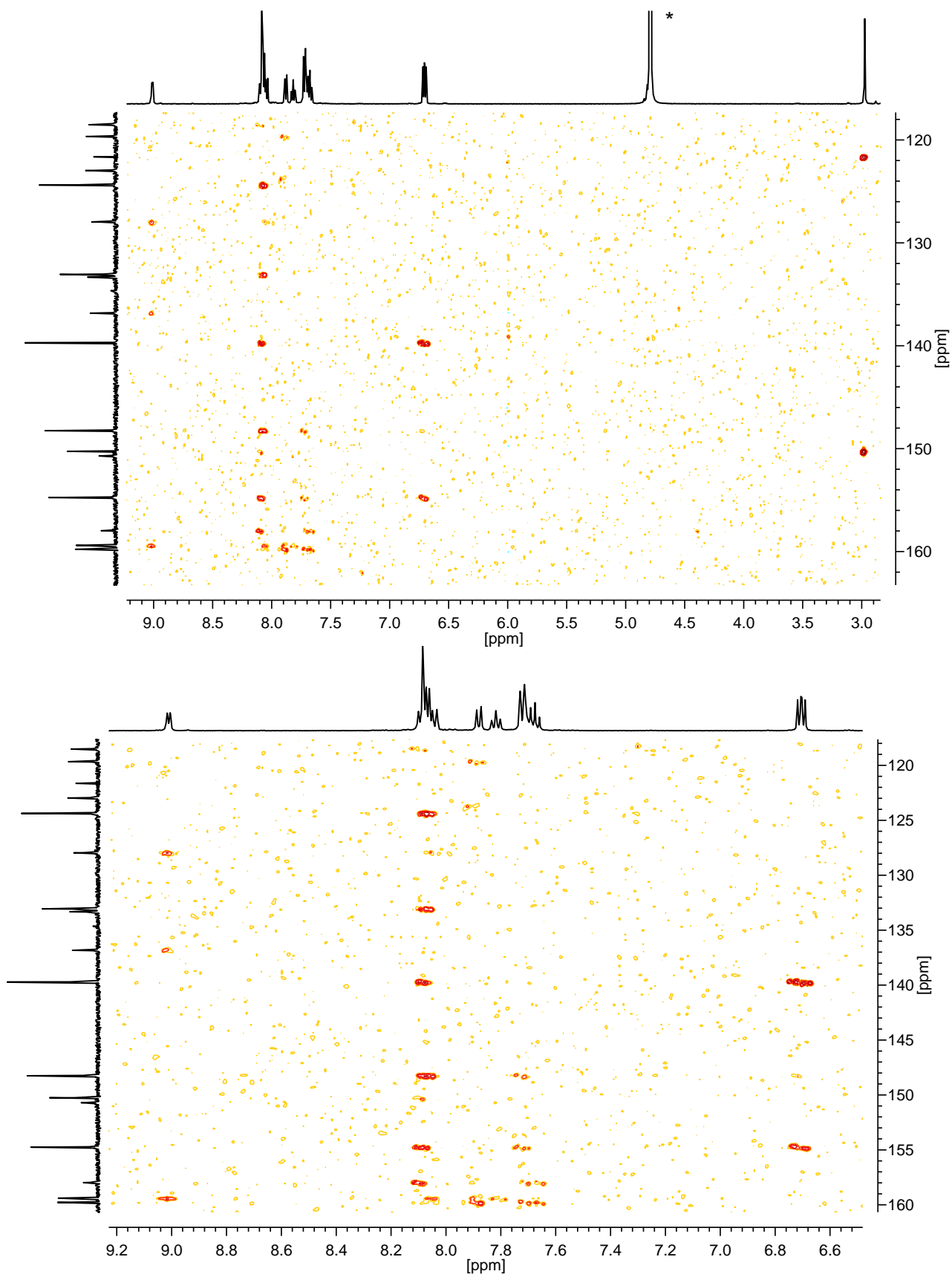


Figure S6: ^1H - ^{13}C -HMBC spectrum of $\text{Na}_3\{1(\text{OH})_2\}$ in D_2O at 299 K (* H_2O). The lower part shows an expansion of the 6.4 – 9.2 ppm region (^1H).

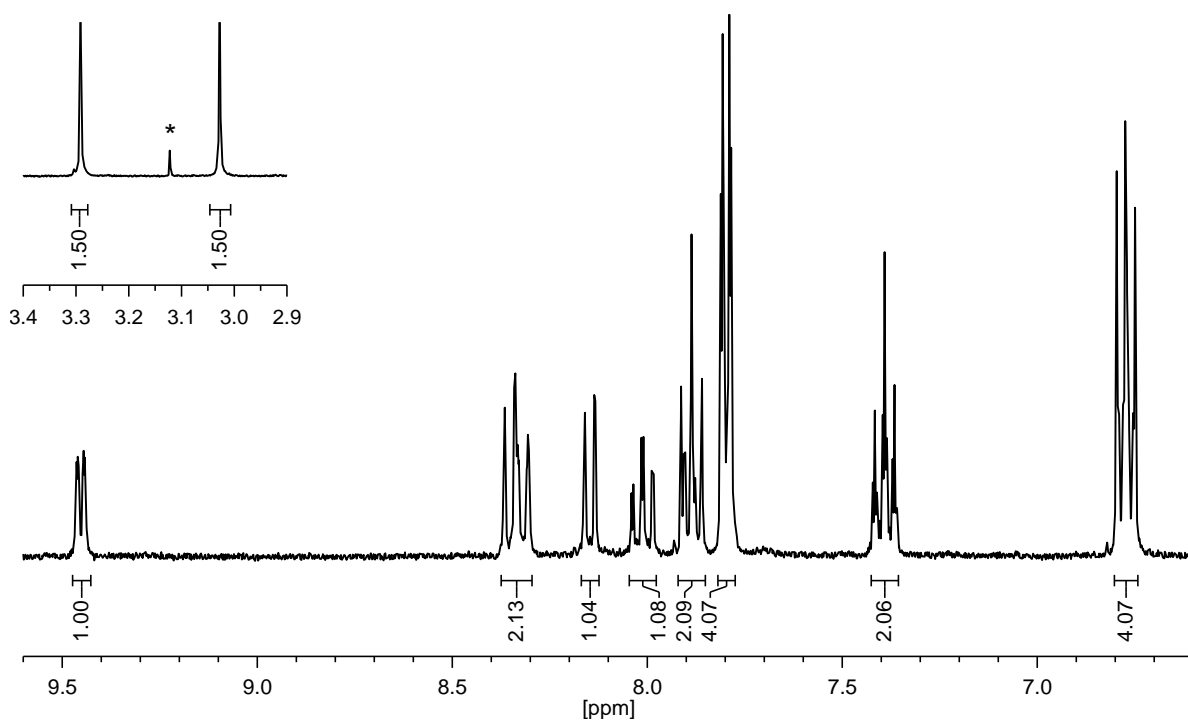


Figure S7: $^1\text{H-NMR}$ spectrum (300 MHz) of $2(\text{PF}_6)_2$ in acetone- d_6 at 299 K (* methyl *tert*-butyl ether).

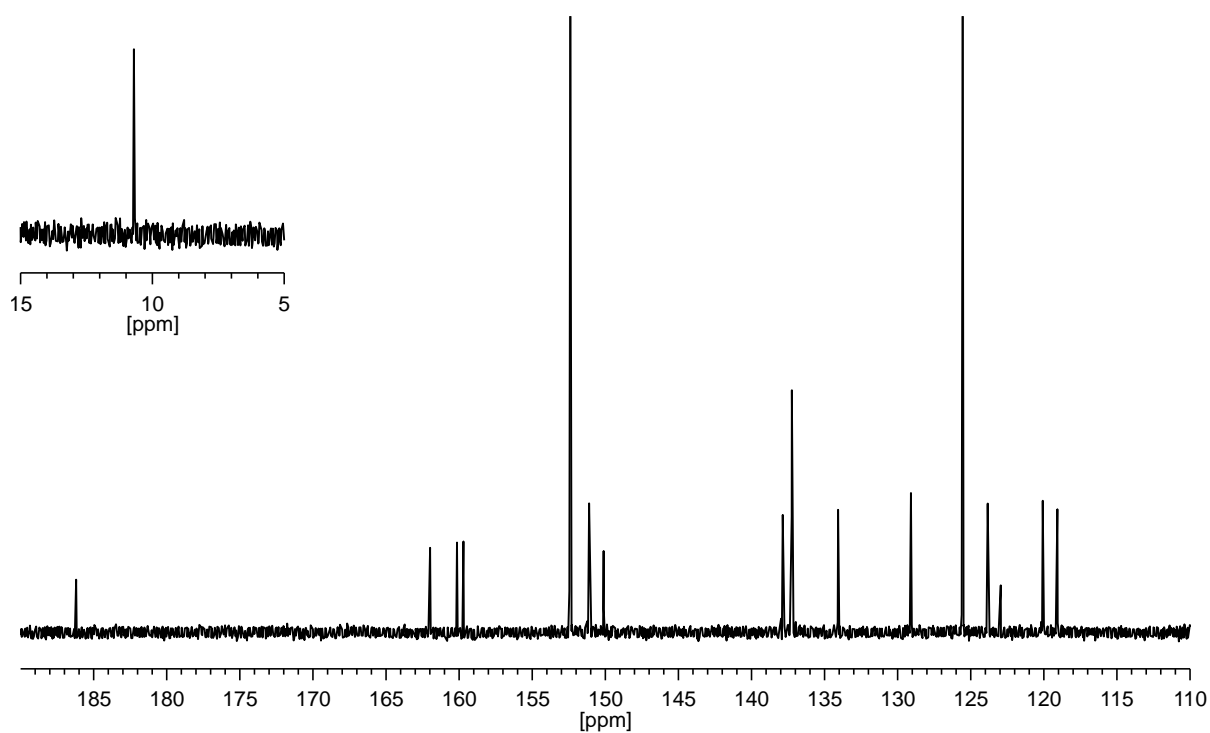


Figure S8: $^{13}\text{C-NMR}$ spectrum (75.5 MHz) of $2(\text{PF}_6)_2$ in acetone- d_6 at 299 K. Signal for the methyl group of the acetate is hidden under the solvent signal (not shown).

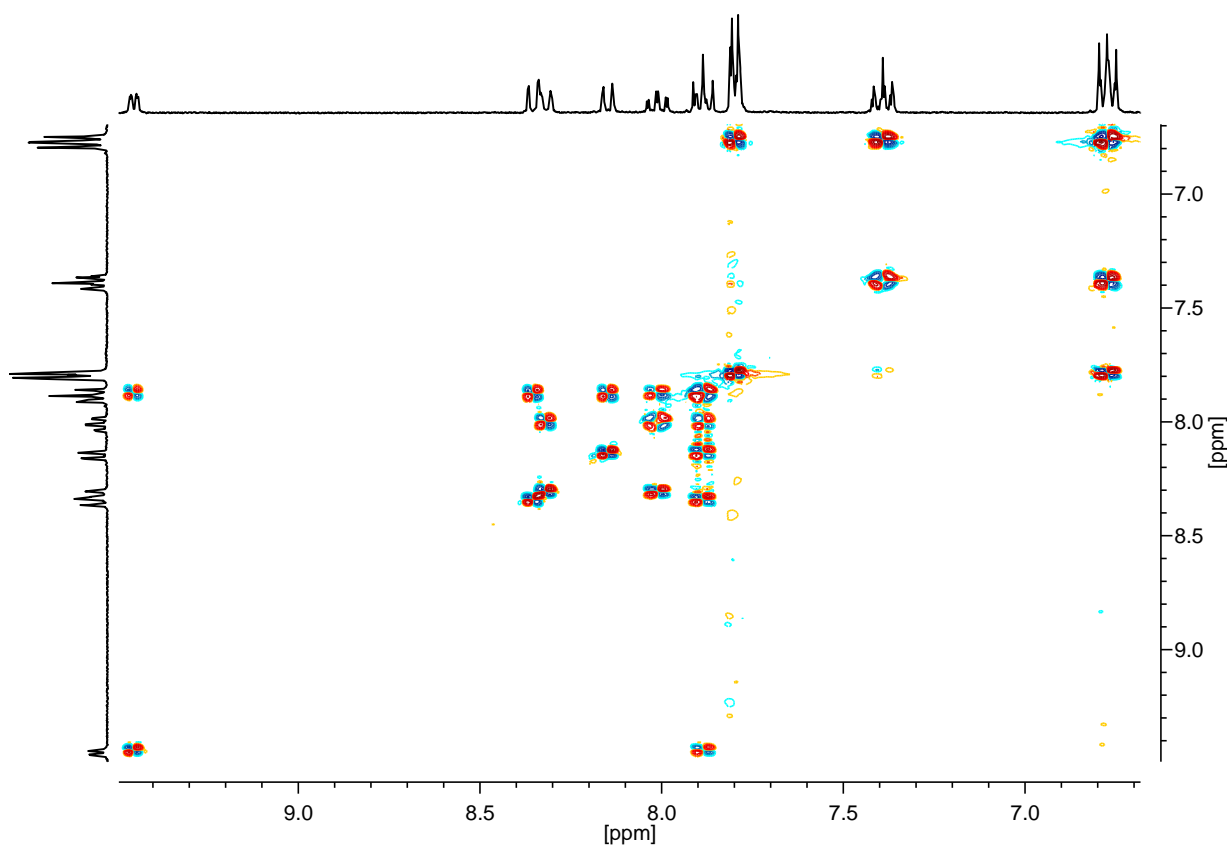


Figure S9: ^1H - ^1H -COSY spectrum of $2(\text{PF}_6)_2$ in acetone- d_6 at 298 K.

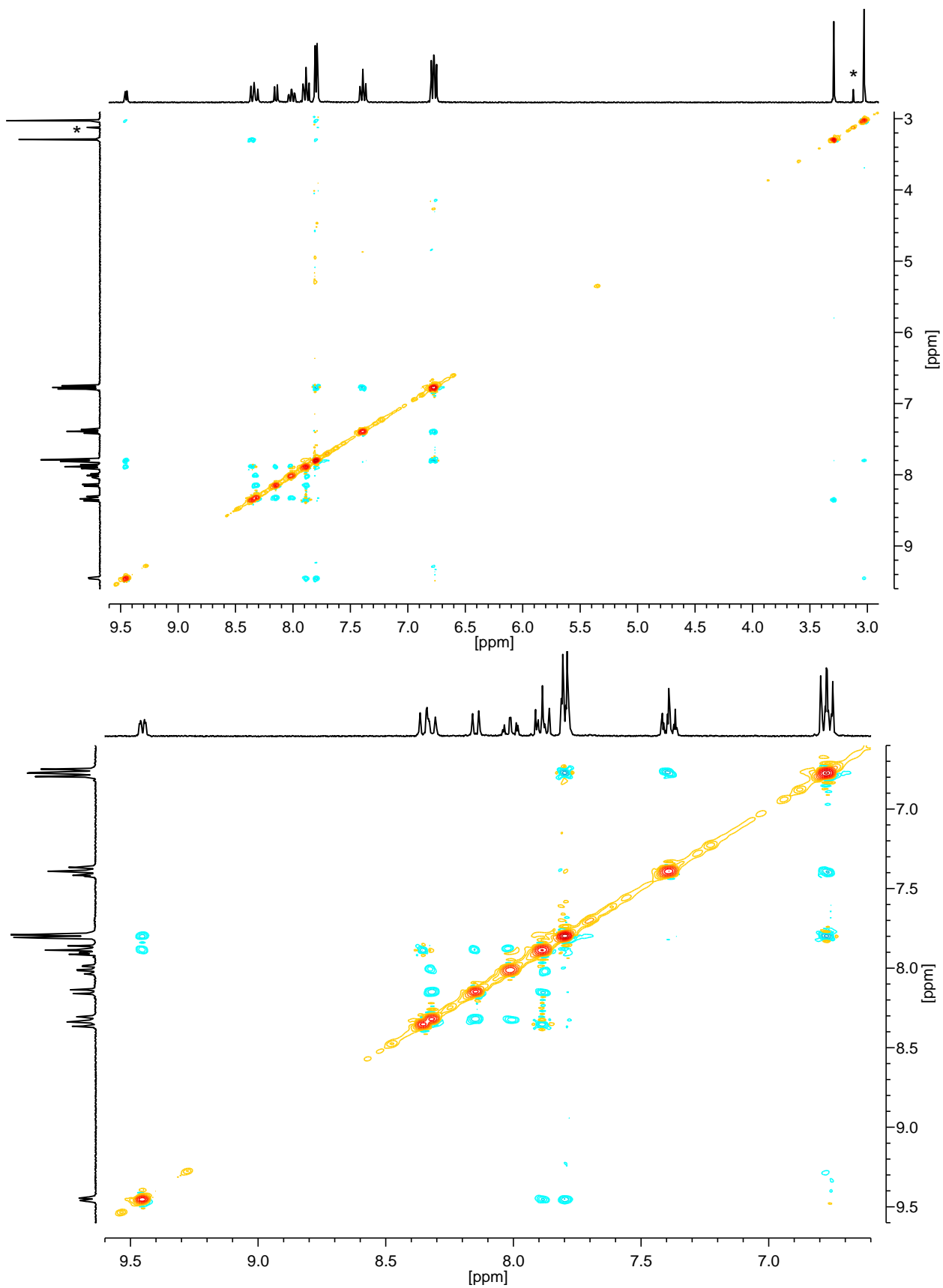


Figure S10: ^1H - ^1H -NOESY spectrum of $2(\text{PF}_6)_2$ in acetone- d_6 at 298 K (* methyl *tert*-butyl ether). The lower part shows an expansion of the 6.6 – 9.6 ppm region.

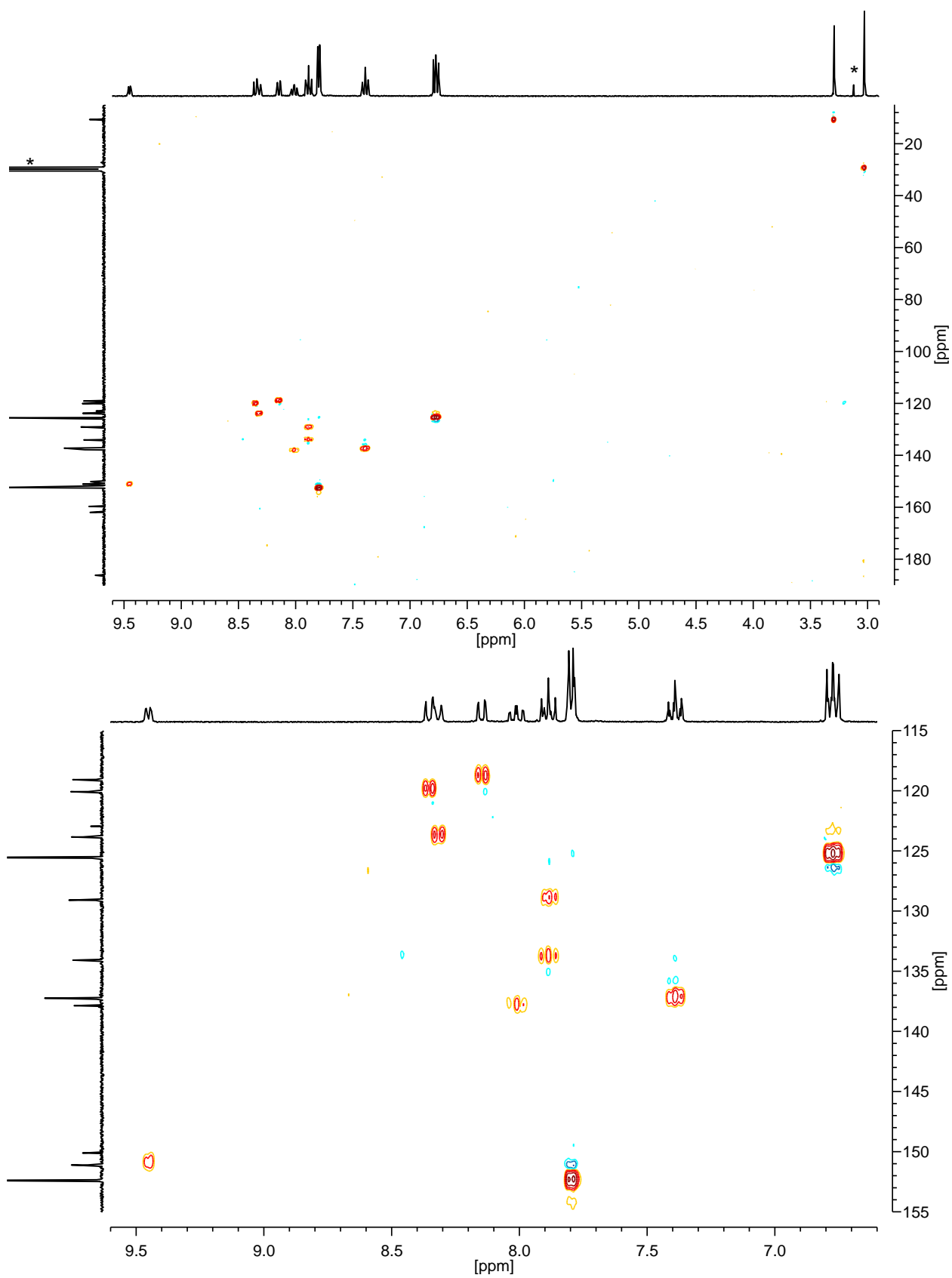


Figure S11: ^1H - ^{13}C -HSQC spectrum of $2(\text{PF}_6)_2$ in acetone- d_6 at 299 K (* methyl *tert*-butyl ether and acetone). The lower part shows an expansion of the 6.6 – 9.6 ppm region (^1H).

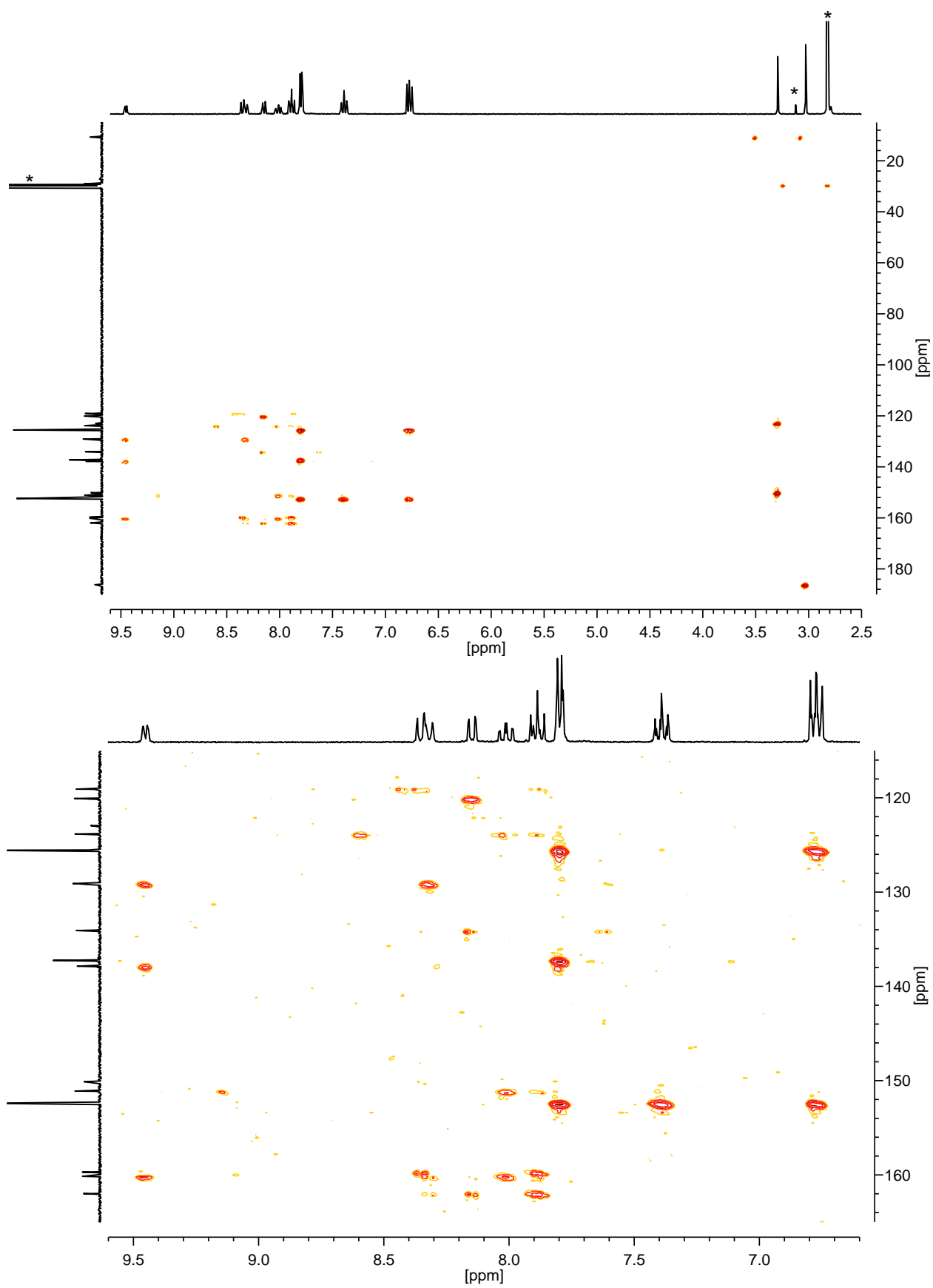


Figure S12: ^1H - ^{13}C -HMBC spectrum of $2(\text{PF}_6)_2$ in acetone- d_6 at 299 K (* methyl *tert*-butyl ether and acetone). The lower part shows an expansion of the 6.5 – 9.1 ppm region (^1H).

Electrochemistry

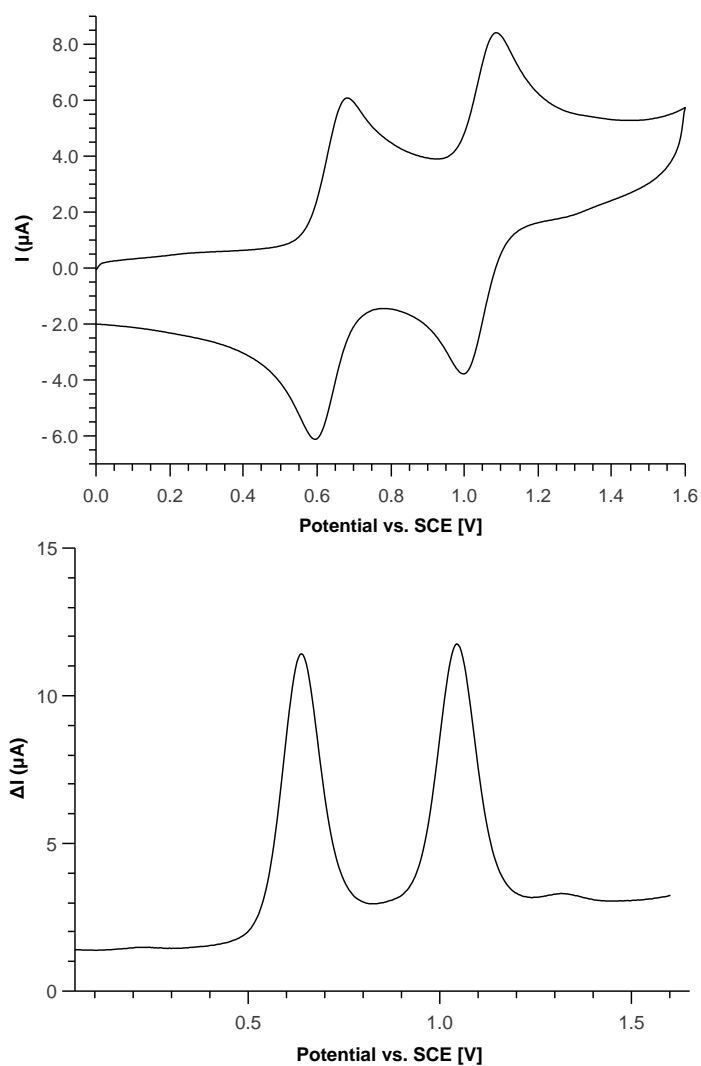


Figure S13: Cyclic voltammogram (top) and Square Wave Voltammogram (bottom) of complex 2^{2+} in Propylene carbonate ($c = 0.1 \text{ mol} \cdot \text{L}^{-1}$ $[\text{N}^{\text{t}}\text{Bu}_4]\text{PF}_6$) on a glassy carbon disk working electrode with Pt wire as auxiliary and SCE reference electrode. (CV: Scan rate = 100 mVs^{-1} , SWV: Scan rate = 4 mVs^{-1} , Pulse Height = 33 mV, Pulse Width = 500 ms, Step Height = 4 mV).

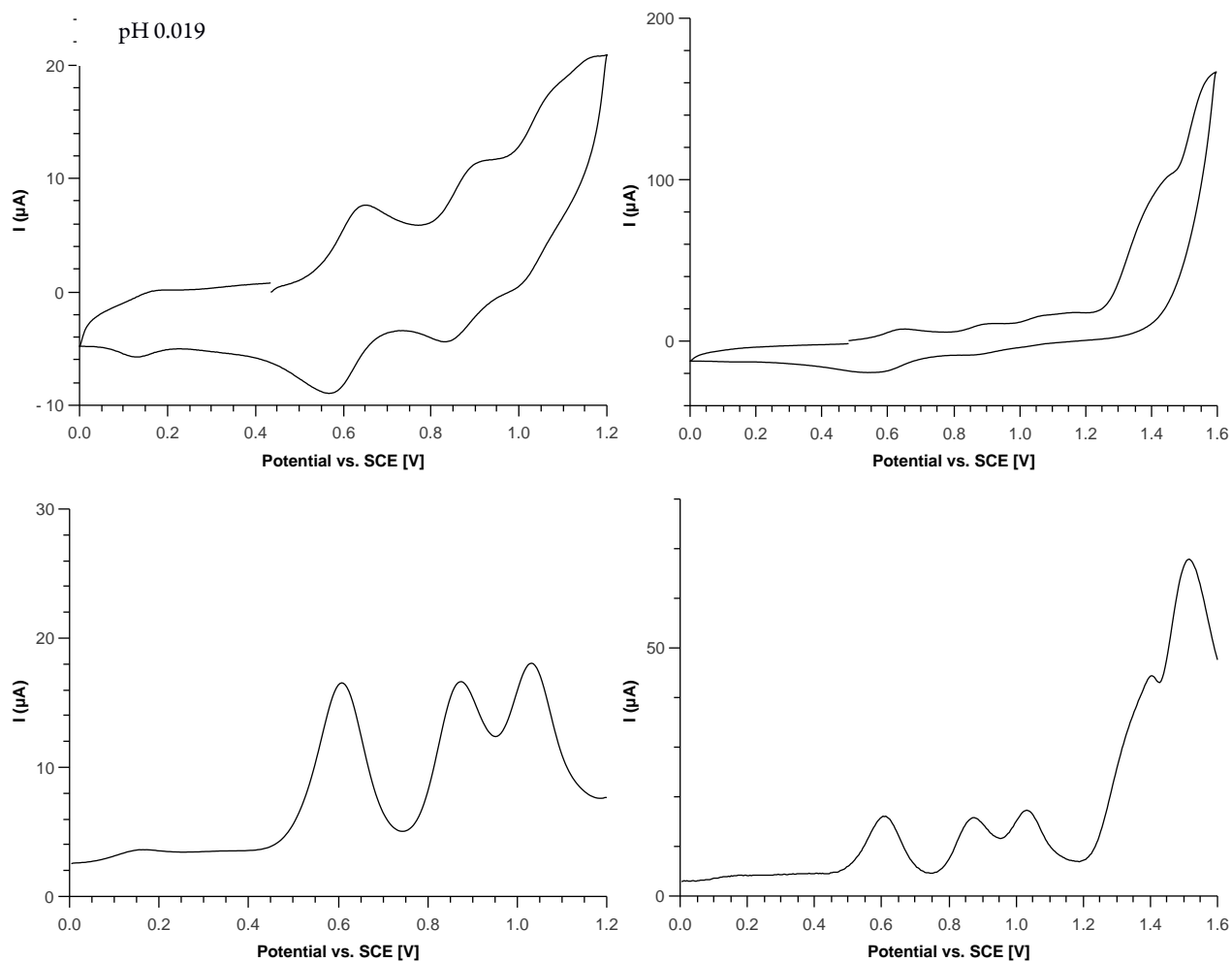


Figure S14: Cyclic Voltammogram (top) and Square Wave Voltammogram (bottom) for different potential ranges (left: 0.0 to 1.2 V, right: 0.0 to 1.6 V) of complex $\{1(\text{H}_2\text{O})_2\}^+$ in aqueous triflic acid (pH 0.019) on a glassy carbon disk working electrode with Pt wire as auxiliary and SCE as reference electrodes. (CV: Scan rate = 100 mVs^{-1} , SWV: Scan rate = 20 mVs^{-1} , Pulse Height = 33 mV, Pulse Width = 100 ms, Step Height = 4 mV).

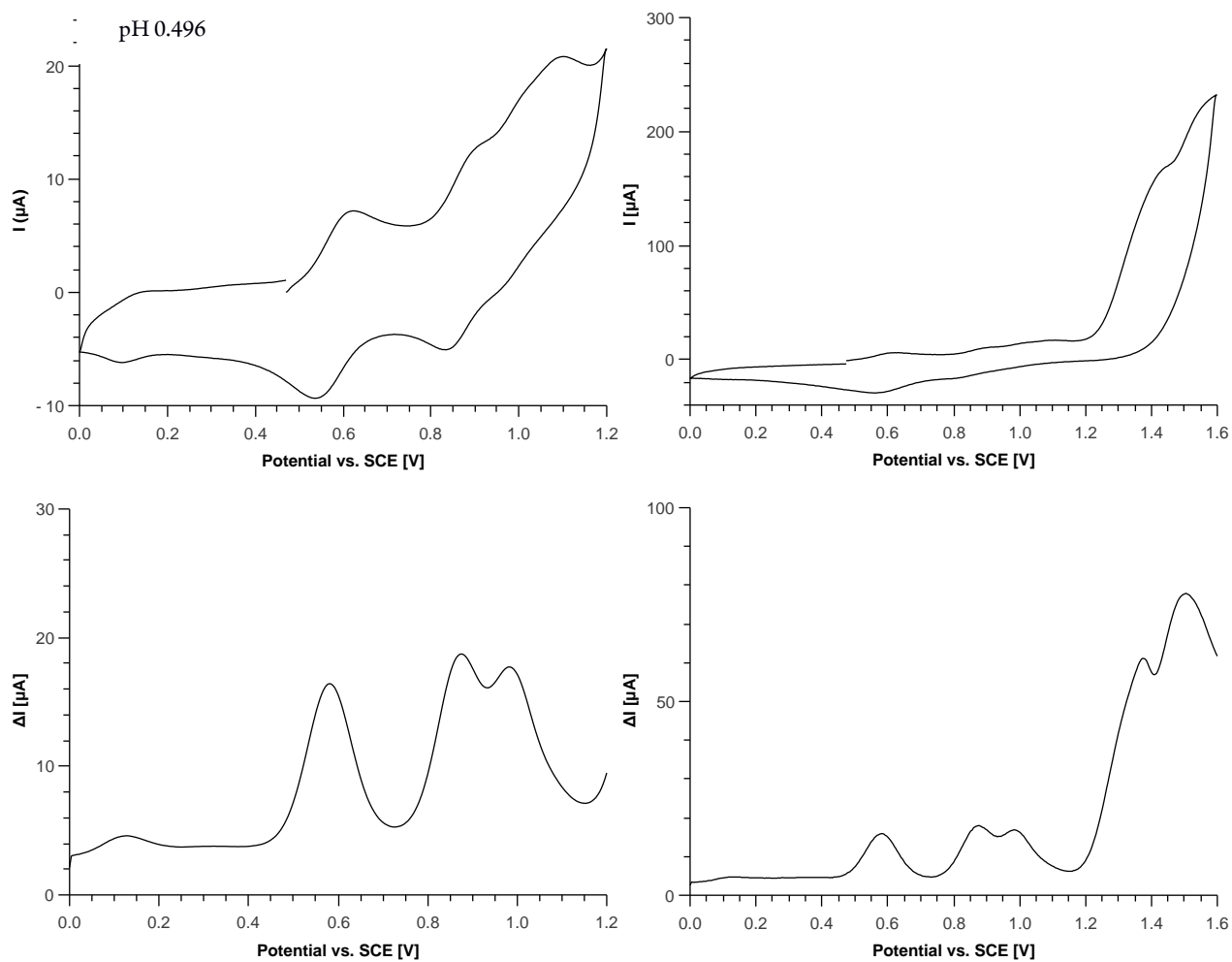


Figure S15: Cyclic Voltammogram (top) and Square Wave Voltammogram (bottom) for different potential ranges (left: 0.0 to 1.2 V, right: 0.0 to 1.6 V) of complex $\{1(\text{H}_2\text{O})_2\}^+$ in aqueous triflic acid (pH 0.496) on a glassy carbon disk working electrode with Pt wire as auxiliary and SCE as reference electrodes. (CV: Scan rate = 100 mVs^{-1} , SWV: Scan rate = 20 mVs^{-1} , Pulse Height = 33 mV, Pulse Width = 100 ms, Step Height = 4 mV).

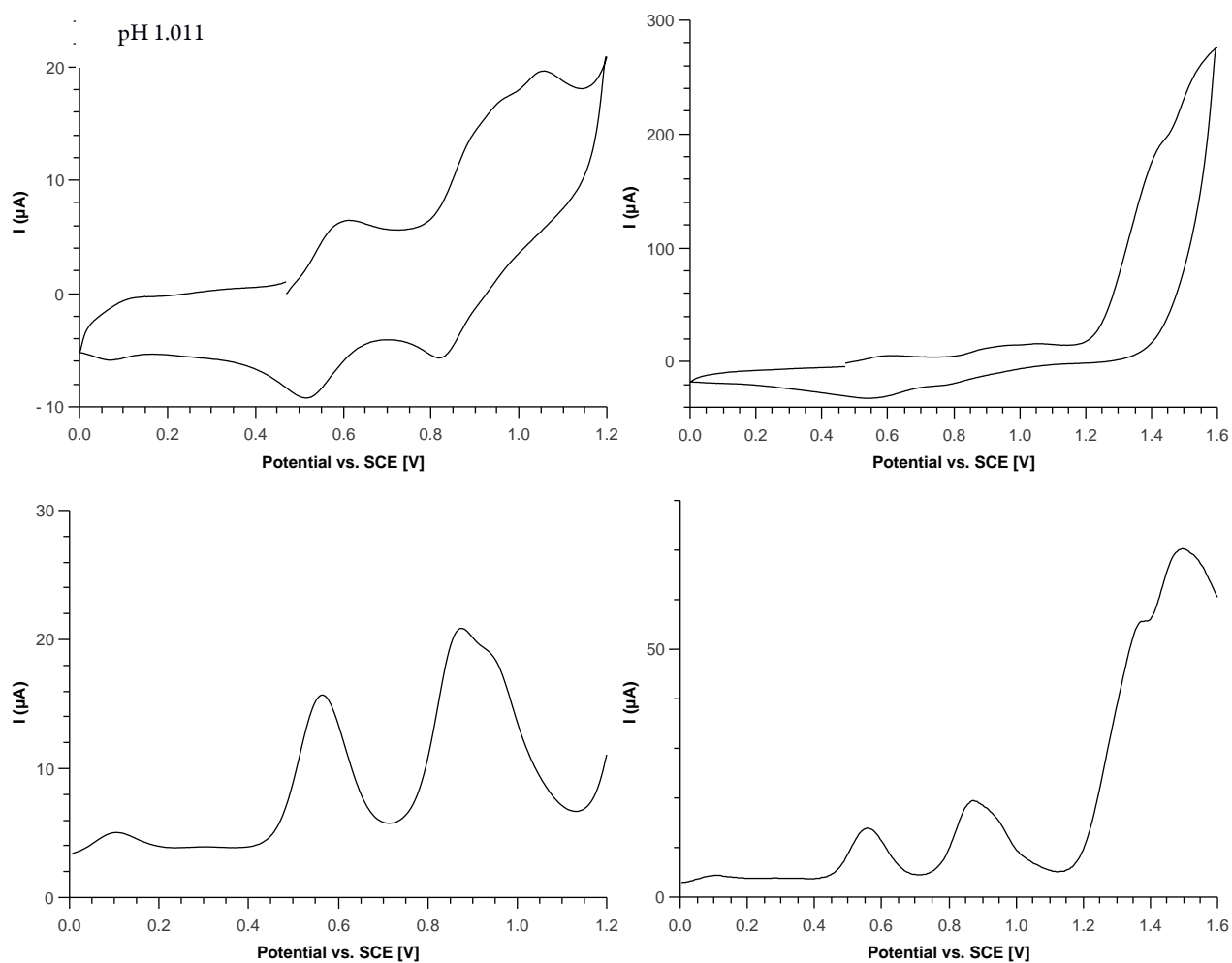


Figure S16: Cyclic Voltammogram (top) and Square Wave Voltammogram (bottom) for different potential ranges (left: 0.0 to 1.2 V, right: 0.0 to 1.6 V) of complex $\{1(H_2O)_2\}^+$ in aqueous triflic acid (pH 1.011) on a glassy carbon disk working electrode with Pt wire as auxiliary and SCE as reference electrodes. (CV: Scan rate = 100 mVs⁻¹, SWV: Scan rate = 20 mVs⁻¹, Pulse Height = 33 mV, Pulse Width = 100 ms, Step Height = 4 mV).

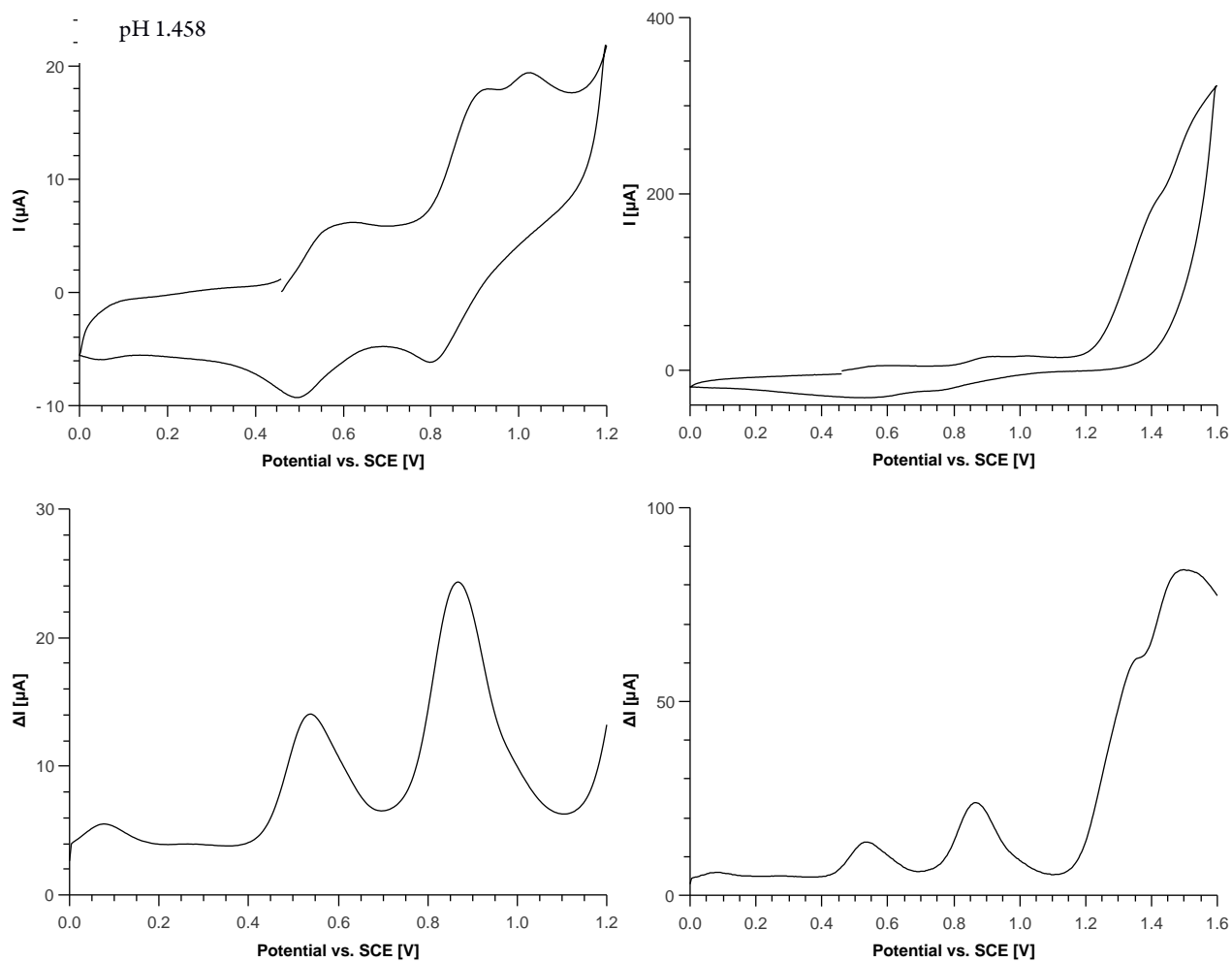


Figure S17: Cyclic Voltammogram (top) and Square Wave Voltammogram (bottom) for different potential ranges (left: 0.0 to 1.2 V, right: 0.0 to 1.6 V) of complex $\{1(\text{H}_2\text{O})_2\}^+$ in aqueous triflic acid (pH 1.458) on a glassy carbon disk working electrode with Pt wire as auxiliary and SCE as reference electrodes. (CV: Scan rate = 100 mVs^{-1} , SWV: Scan rate = 20 mVs^{-1} , Pulse Height = 33 mV, Pulse Width = 100 ms, Step Height = 4 mV).

Spectrophotometric Redox Titration

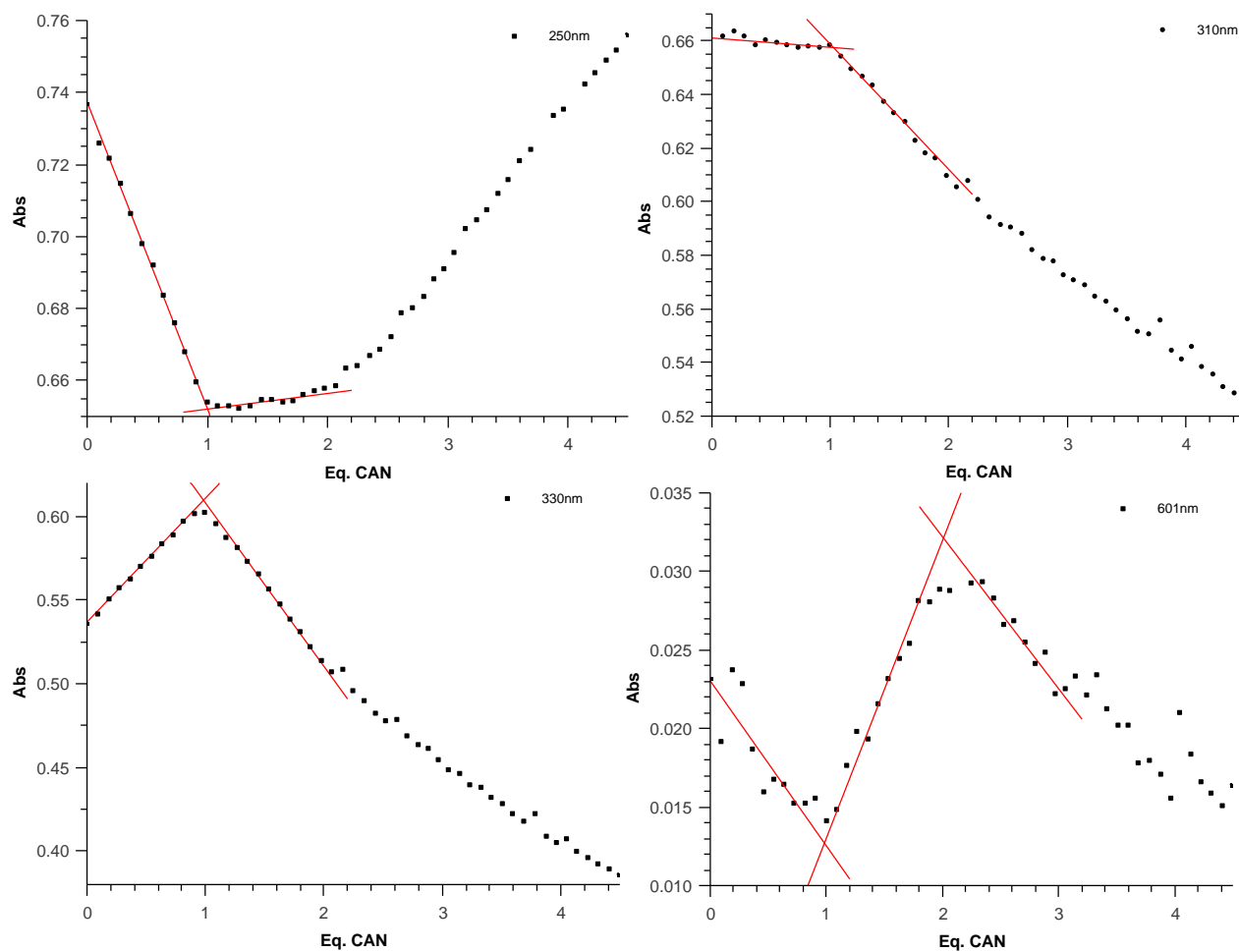


Figure S18: Spectrophotometric redox titration of complex $\{1(\text{H}_2\text{O})_2\}^-$ ($c = 2.40 \cdot 10^{-5} \text{ mol} \cdot \text{L}^{-1}$) with Ce(IV) in aqueous triflic acid ($c = 0.1 \text{ mol} \cdot \text{L}^{-1}$, pH 1). Each addition corresponds to 0.09 equivalents of oxidant. Plot of absorbance vs. equivalents of Ce(IV) for selected wavelength (top left: 250 nm, top right: 310 nm, bottom left: 330 nm and bottom right: 601 nm). Linear curve fitting (red) were used to calculate the exact number of equivalents.

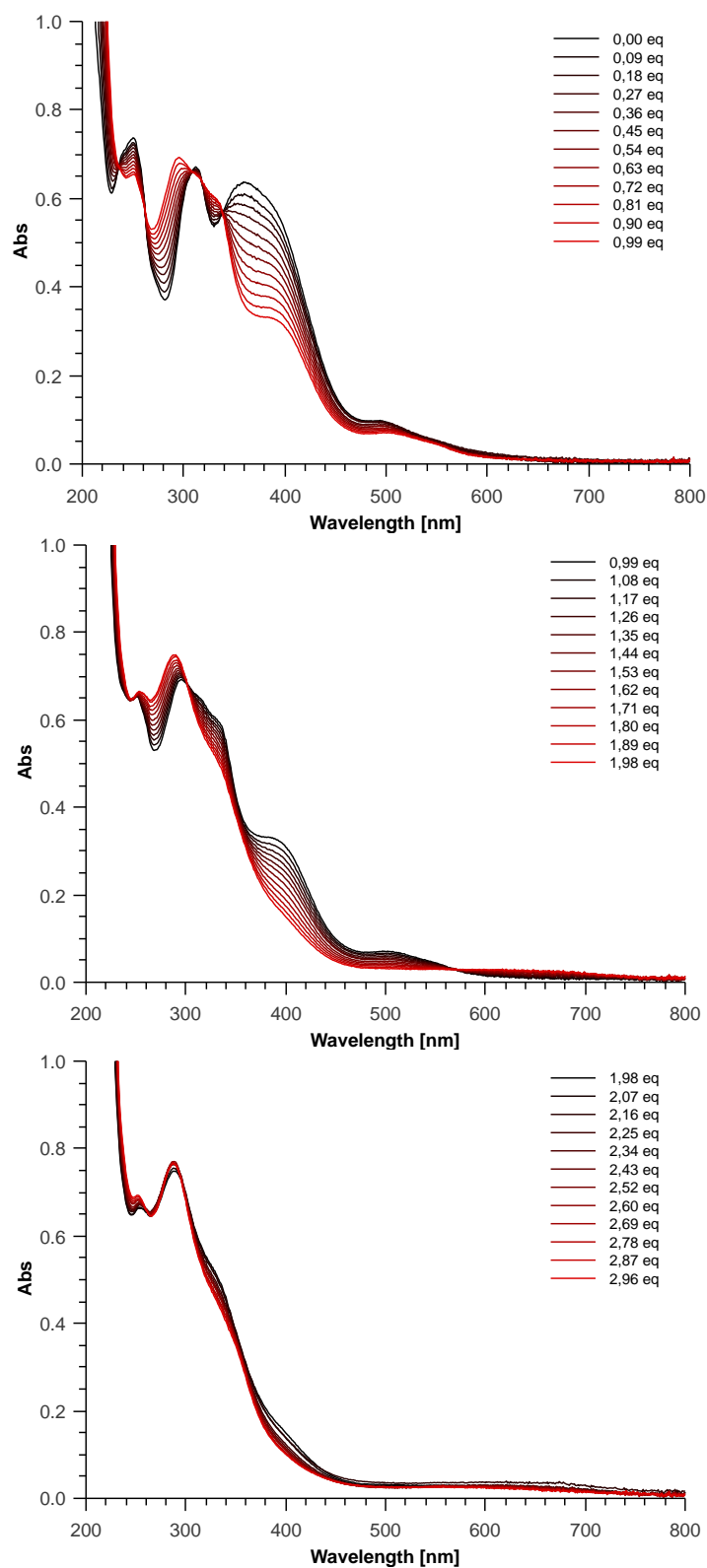


Figure S19: Spectrophotometric redox titration of complex $\{1(\text{H}_2\text{O})_2\}^-$ ($c = 2.40 \cdot 10^{-5} \text{ mol} \cdot \text{L}^{-1}$) with Ce(IV) in aqueous triflic acid ($c = 0.1 \text{ mol} \cdot \text{L}^{-1}$, pH 1). Each addition corresponds to 0.09 equivalents of oxidant. Spectral changes for the first (top, isosbestic points at 236, 262, 308, 318 and 339 nm), second (middle, isosbestic points at 301 and 570 nm) and third oxidation (bottom, isosbestic point at 300 nm).

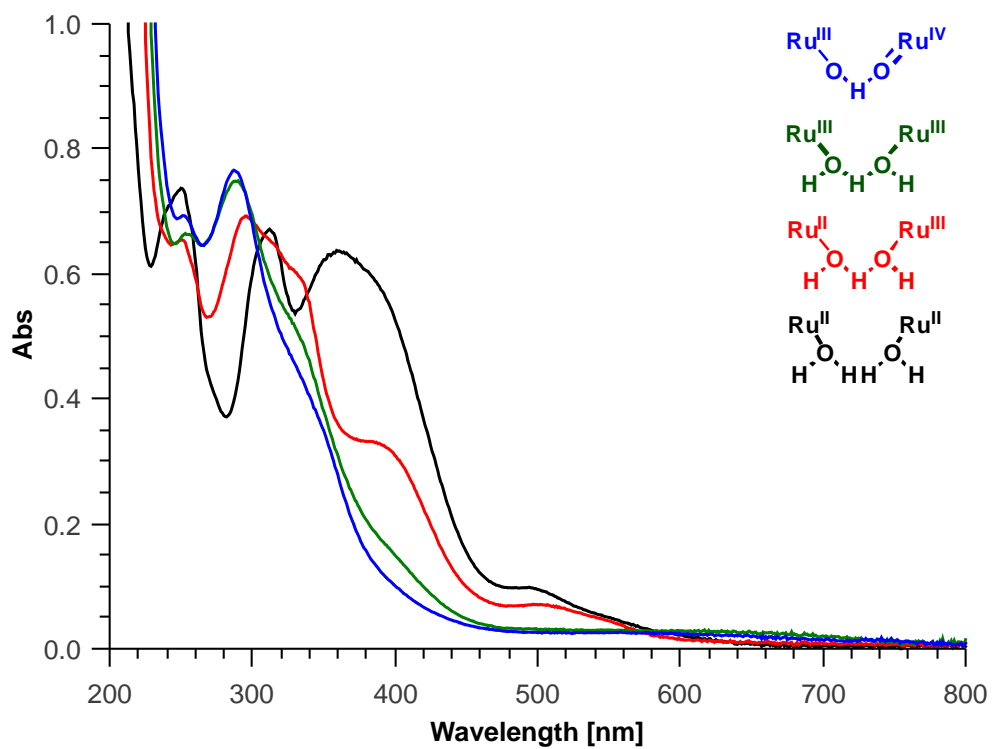


Figure S20: UV-vis spectrum for $\{\mathbf{1}(\text{H}_2\text{O})_2\}^-$ and three consecutively one-electron oxidized products in aqueous triflic acid ($c = 0.1 \text{ mol} \cdot \text{L}^{-1}$, pH 1) derived from spectrophotometric redox titration.

Catalysis Experiments

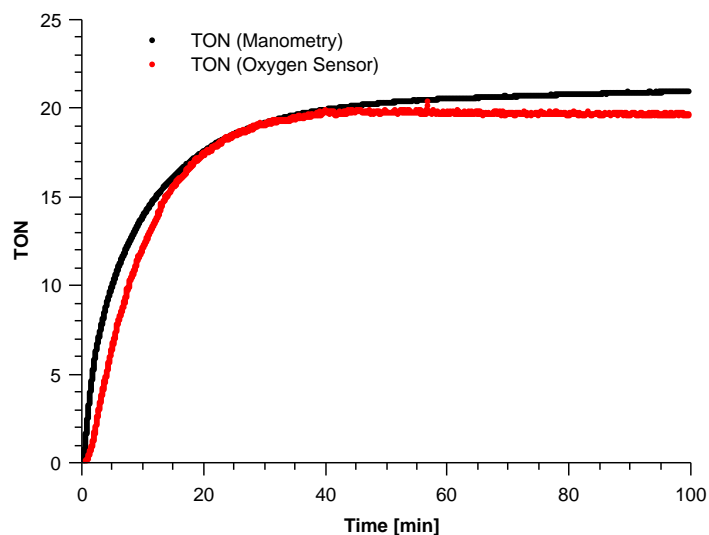


Figure S21: Catalytic activity of complex $\{1(\text{H}_2\text{O})_2\}^-$ ($c = 1.0 \times 10^{-3} \text{ mol} \cdot \text{L}^{-1}$) in aqueous triflic acid ($c = 0.1 \text{ mol} \cdot \text{L}^{-1}$, pH 1) with 100 equivalents of Ce(IV). Oxygen evolution was monitored by on-line manometry and a gas phase Clark Electrode.

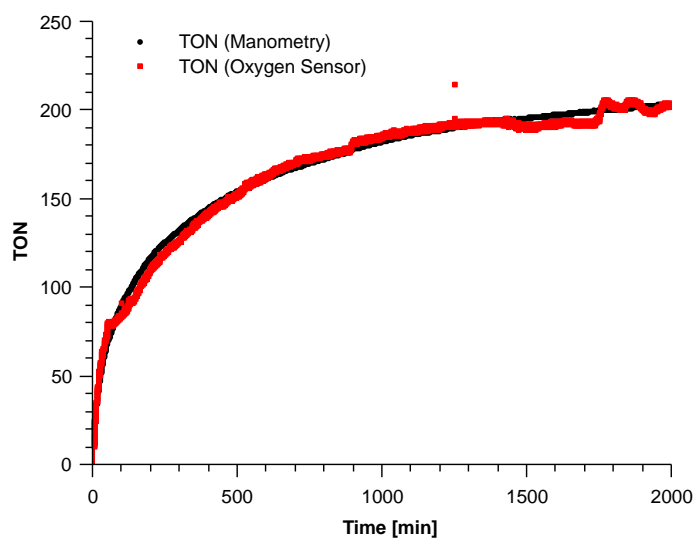


Figure S22: Catalytic activity of complex $\{1(\text{H}_2\text{O})_2\}^-$ ($c = 9.4 \times 10^{-5} \text{ mol} \cdot \text{L}^{-1}$) in aqueous triflic acid ($c = 0.1 \text{ mol} \cdot \text{L}^{-1}$, pH 1) with 1000 equivalents of Ce(IV). Oxygen evolution was monitored by on-line manometry and a gas phase Clark Electrode.

Exchange Kinetics

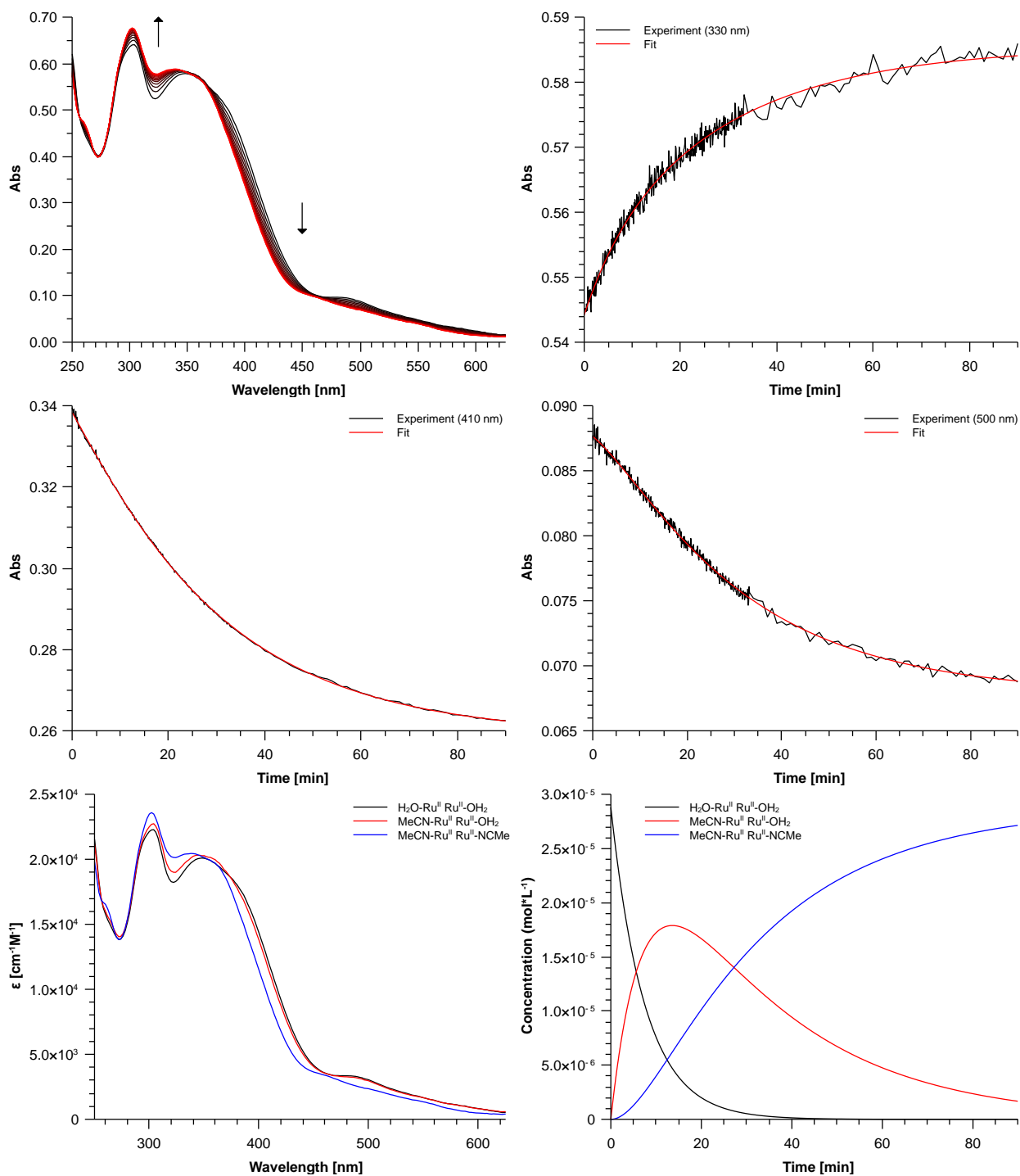


Figure S23: Exchange kinetics of complex $\{1(\text{H}_2\text{O})_2\}^-$ ($c = 2.87 \cdot 10^{-5} \text{ mol} \cdot \text{L}^{-1}$) in oxidation state II,II with acetonitrile under pseudo first order conditions in aqueous triflic acid ($c = 0.1 \text{ mol} \cdot \text{L}^{-1}$, pH 1) at 25.0 °C. Spectral changes in the UV-vis region (top left), experimental and calculated kinetic traces for selected wavelength (top right: 330 nm, middle left: 410 nm, middle right: 500 nm) as well as calculated spectra of single compounds (bottom left) and the calculated species distribution diagram (bottom right) are shown.

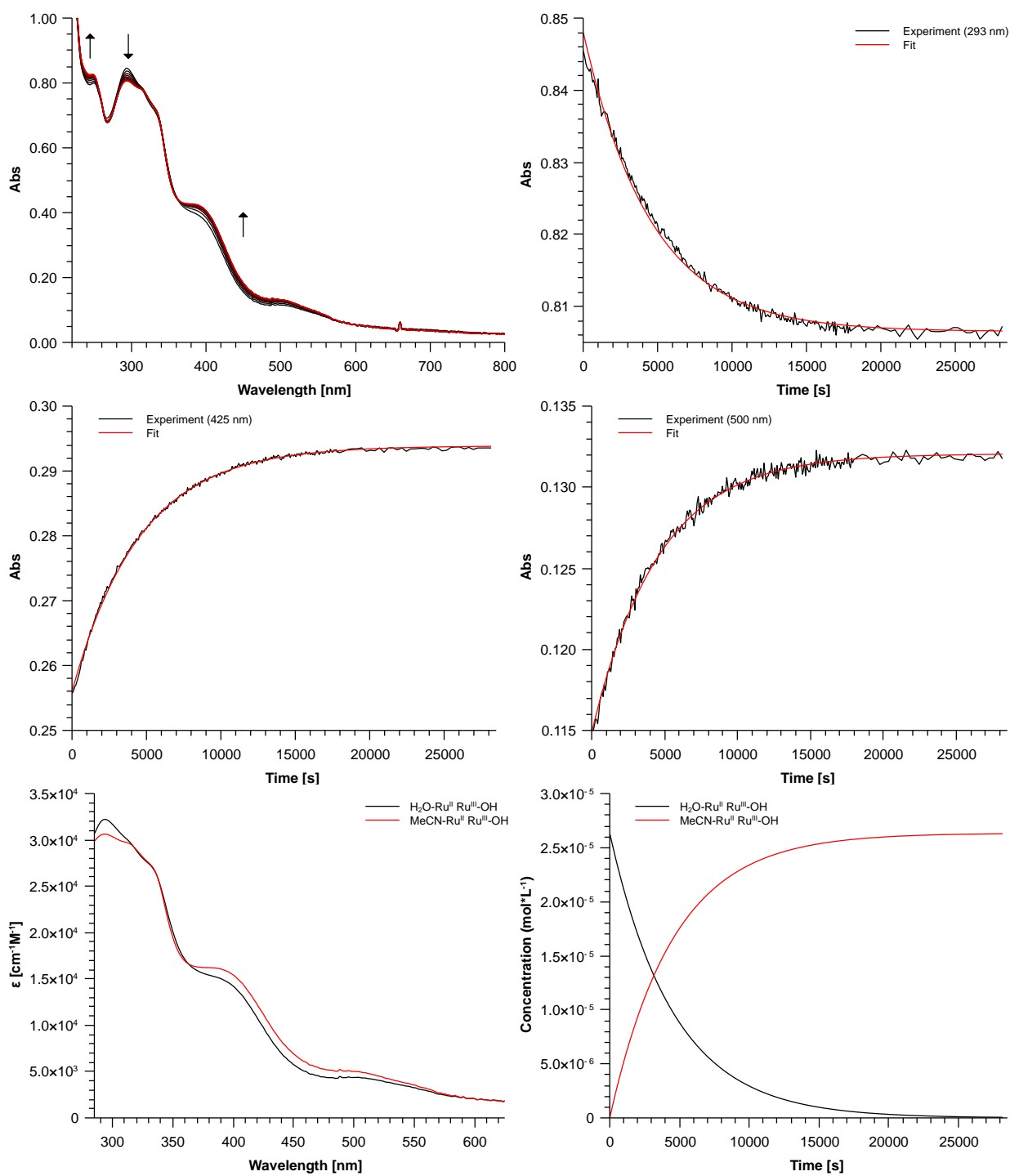


Figure S24: Exchange kinetics of complex $\{1(\text{H}_2\text{O})_2\}^-$ ($c = 2.63 \cdot 10^{-5} \text{ mol} \cdot \text{L}^{-1}$) in oxidation state III,II with acetonitrile under pseudo first order conditions in aqueous triflic acid ($c = 0.1 \text{ mol} \cdot \text{L}^{-1}$, pH 1) at 27.6°C . Spectral changes in the UV-vis region (top left), experimental and calculated kinetic traces for selected wavelength (top right: 293 nm, middle left: 425 nm, middle right: 500 nm) as well as calculated spectra of single compounds (bottom left) and the calculated species distribution diagram (bottom right) are shown.

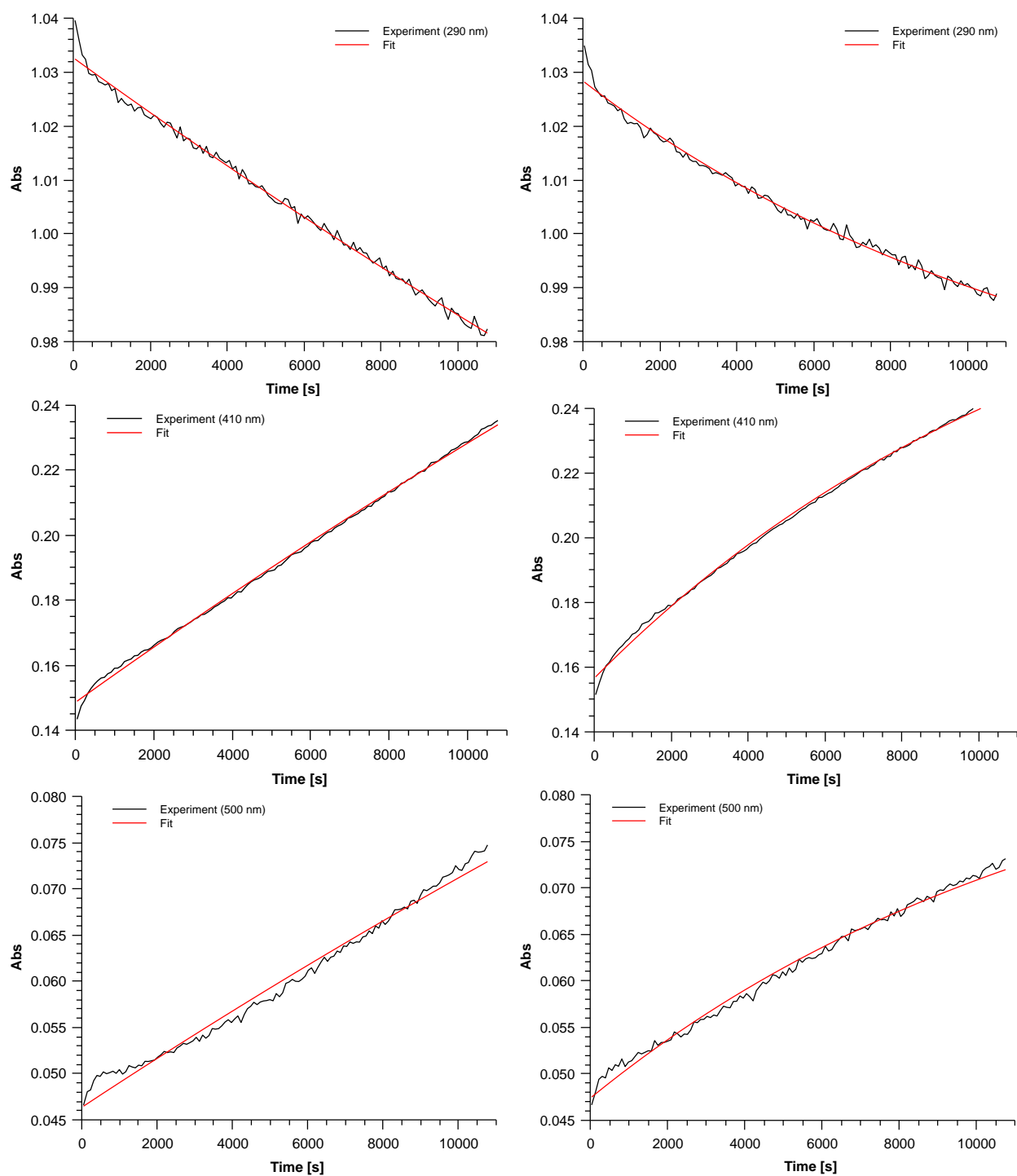


Figure S25: Exchange kinetics (left) of complex $\{1(\text{H}_2\text{O})_2\}^-$ ($c = 3.12 \cdot 10^{-5} \text{ mol} \cdot \text{L}^{-1}$) in oxidation state III,III with acetonitrile under pseudo first order conditions and stability measurements (right) of complex $\{1(\text{H}_2\text{O})_2\}^-$ ($c = 3.14 \cdot 10^{-5} \text{ mol} \cdot \text{L}^{-1}$) in oxidation state III,III both in aqueous triflic acid ($c = 0.1 \text{ mol} \cdot \text{L}^{-1}$, pH 1) at 27.6 °C. Experimental and calculated kinetic traces for selected wavelength (top: 290 nm, middle: 410 nm, bottom: 500 nm) are shown.

Complex	Oxidation state	First substitution k_1 [s ⁻¹]	Second substitution k_2 [s ⁻¹]	T [°C]
$\{1(H_2O)_2\}^-$	II,II	$2.2 \cdot 10^{-3}$	$5.1 \cdot 10^{-4}$	25.0
	III,II	$2.3 \cdot 10^{-4}$	---	27.6
	III,III	Exchange: $1.9 \cdot 10^{-5}$ Stability: $5.5 \cdot 10^{-5}$	---	27.6
4^{3+} [6]	II,II	$4.0 \cdot 10^{-2}$	$5.8 \cdot 10^{-5}$	25.0
	III,II	$8.8 \cdot 10^{-4}$	---	25.0
	III,III	$2.0 \cdot 10^{-5}$	---	25.0

Table S1: Rate constants for exchange kinetics with acetonitrile of complex $\{1(H_2O)_2\}^-$ in different oxidation states under pseudo first order conditions in aqueous triflic acid (0.1 M, pH 1). Literature^[6] known rate constants for 4^{3+} are shown for comparison.

Comment on exchange kinetics for oxidation state III,III:

For the oxidation state III,III kinetic traces and calculated rate constants for the substitution with acetonitrile and for the decay measurements are very similar. Beside the exchange process in oxidation state III,III (slow) several other processes like reaction of oxidation state III,III (e.g. reduction to III,II - slow) and reaction of decomposition products (e.g. substitution in oxidation state III,II – fast) take place. The rate constant for oxidation state III,III should therefore be considered as rate constant for decomposition and reaction of III,III rather than as a rate constant for substitution only. The argumentation to oxidize the complex to oxidation state III,III for the labelling studies stays the same since the rate constant is much lower compared to the ones obtained for oxidation state II,II and III,II.

Labeling Experiments

Experiment	¹⁸ O ^a (%)	O ₂	Exch. ^b	WNA ^c	I2M ^d	Exp.
1	Solv: 24.3	³² O ₂	57.3	65.1	73.8	62.3
		³⁴ O ₂	36.8	31.5	24.2	33.2
	Cat: 14.1	³⁶ O ₂	5.9	3.4	2.0	4.5
		³² O ₂ / ³⁴ O ₂	1.6	2.1	3.1	1.9
		³⁴ O ₂ / ³⁶ O ₂	6.2	9.2	12.2	7.3
2	Solv: 48.6	³² O ₂	26.4	1.5	0.1	6.1 ^e
		³⁴ O ₂	50.0	51.3	5.8	52.6
	Cat: 97.0	³⁶ O ₂	23.6	47.1	94.1	41.3
		³² O ₂ / ³⁴ O ₂	0.5	3.0 e-02	1.5 e-02	0.1 ^e
		³⁴ O ₂ / ³⁶ O ₂	2.1	1.1	0.1	1.3

Table S2: Relative isotopic ratios of O₂ evolved from the first catalytic cycle at different degree of catalyst and solvent ¹⁸O labeling, together with expected values calculated for different reaction mechanisms.

^a Degree of solvent (Solv.) and catalyst (Cat.) ¹⁸O labeling (%). ^b Exch.: expected ratios in the case of a fast O atom exchange between the catalyst and the solvent. ^c WNA: expected ratios for the mechanism involving a nucleophilic attack of a solvent water to the O atom of a Ru-O group. ^d I2M: expected ratios for an intramolecular mechanism involving an oxygen-oxygen coupling from two Ru-O groups. ^e Trace contamination with air during Ce(IV) addition is responsible for the inaccuracy of the ³²O₂ values.

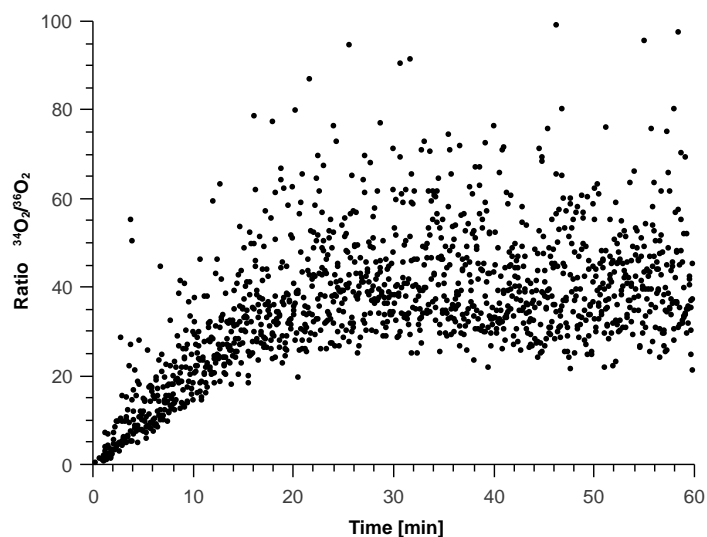


Figure S26: Evolution of the $^{34}\text{O}_2/^{36}\text{O}_2$ ratio obtained by MS for the experiment in Table 2 (main article). Online oxygen evolution profiles and evolution of the $^{32}\text{O}_2/^{34}\text{O}_2$ ratio are shown in the main article (Figure 3). Traces were obtained by addition of 4 equivalents of Ce(IV) dissolved in degassed aqueous triflic acid ($c = 0.1 \text{ mol}\cdot\text{L}^{-1}$, pH 1) in 97.0 % labeled H_2^{18}O , to a solution of $\{\mathbf{1}(\text{H}_2\text{O})_2\}^-$ at oxidation state III,III dissolved in degassed aqueous triflic acid ($c = 0.1 \text{ mol}\cdot\text{L}^{-1}$, pH 1) in 0.2 % labeled H_2^{18}O (final solution contains 0.2 % ^{18}O labeled catalyst and 12.3 % H_2^{18}O). The intensity of the $^{36}\text{O}_2$ trace is very low which leads to a large error.

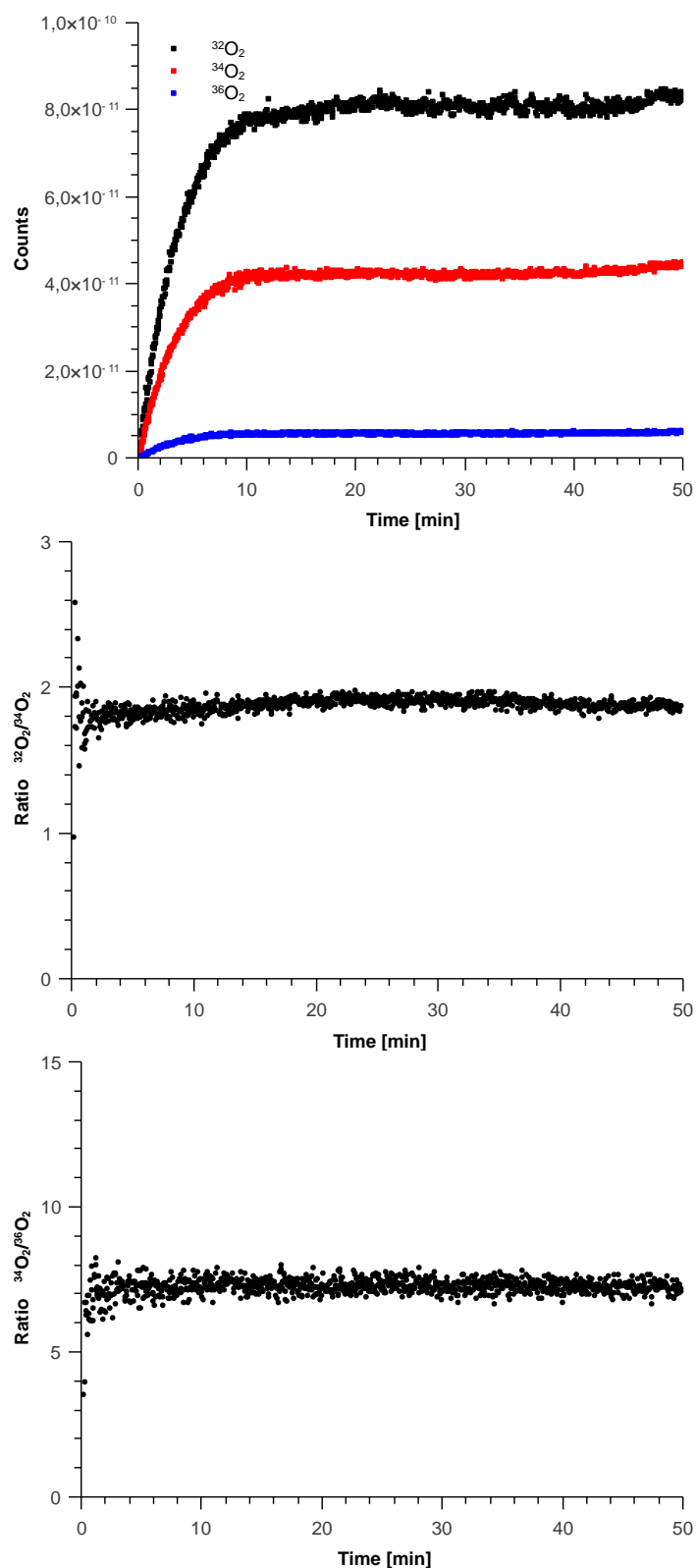


Figure S27: Online oxygen evolution profiles (top), evolution of the $^{32}\text{O}_2/^{34}\text{O}_2$ (middle) and $^{34}\text{O}_2/^{36}\text{O}_2$ ratio (bottom) obtained by MS for the first experiment in Table S2 (SI). Traces were obtained by addition of 4 equivalents of Ce(IV) dissolved in degassed aqueous triflic acid ($c = 0.1 \text{ mol} \cdot \text{L}^{-1}$, pH 1) in 97.0 % labeled H_2^{18}O , to a solution of $\{\mathbf{1}(\text{H}_2\text{O})_2\}^-$ at oxidation state III,III dissolved in degassed aqueous triflic acid ($c = 0.1 \text{ mol} \cdot \text{L}^{-1}$, pH 1) in 14,1 % labeled H_2^{18}O (final solution contains 14.1 % ^{18}O labeled catalyst and 24.3 % H_2^{18}O).

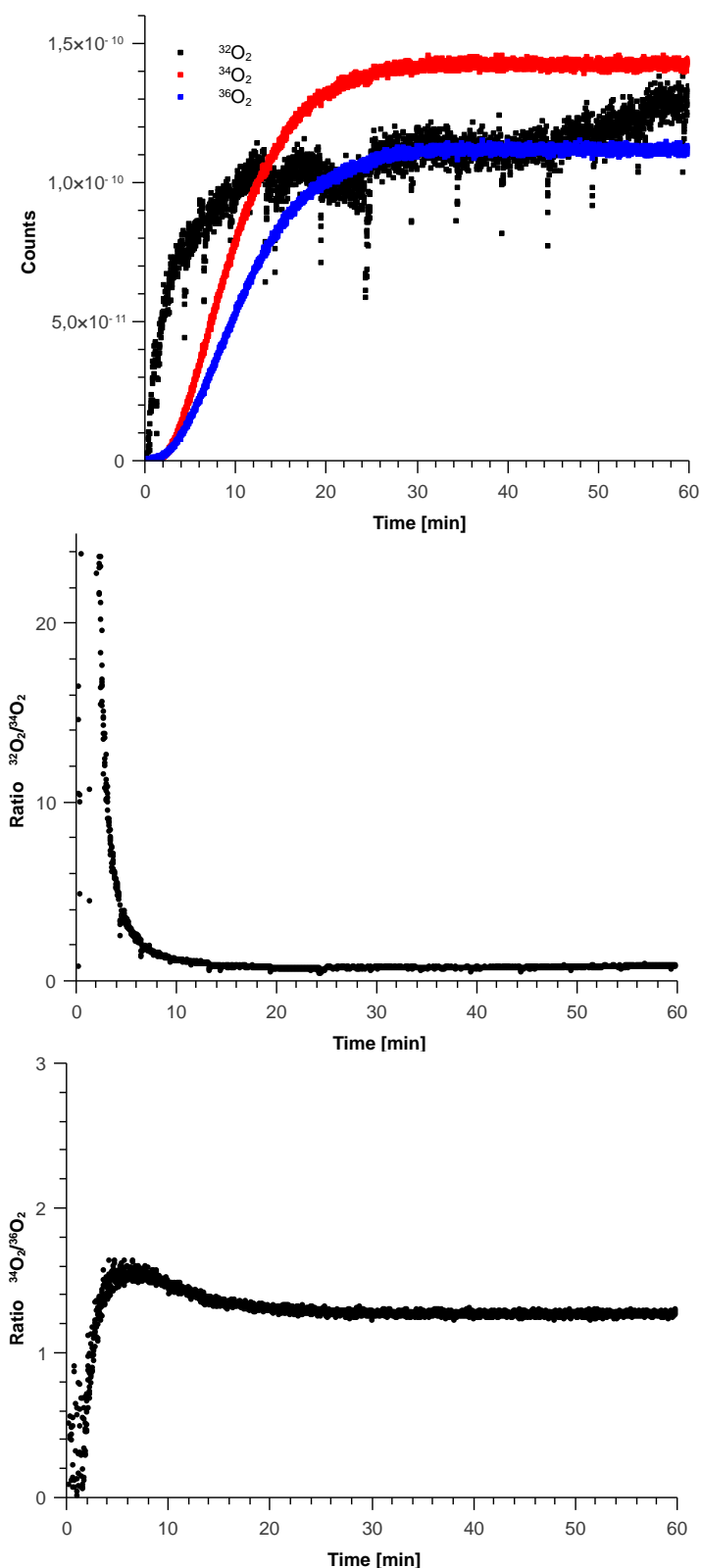


Figure S28: Online oxygen evolution profiles (top), evolution of the $^{32}\text{O}_2/^{34}\text{O}_2$ (middle) and $^{34}\text{O}_2/^{36}\text{O}_2$ ratio (bottom) obtained by MS for the second experiment in Table S2 (SI). Traces were obtained by addition of 4 equivalents of Ce(IV) dissolved in degassed aqueous triflic acid ($c = 0.1 \text{ mol}^* \text{L}^{-1}$, pH 1) in 0.2 % labeled H_2^{18}O , to a solution of $\{\mathbf{1}(\text{H}_2\text{O})_2\}^+$ at oxidation state III,III dissolved in degassed aqueous triflic acid ($c = 0.1 \text{ mol}^* \text{L}^{-1}$, pH 1) in 97.0 % labeled H_2^{18}O (final solution contains 97.0 % ^{18}O labeled catalyst and 48.6 % H_2^{18}O). Contamination with air during Ce(IV) addition is responsible for the inaccuracy of the $^{32}\text{O}_2$ values. For Table S2 (SI) the increase of $^{32}\text{O}_2$ trace in the first 8 min was discarded. Thus the $^{32}\text{O}_2$ trace is inaccurate and the $^{34}\text{O}_2$ and $^{36}\text{O}_2$ traces together with their ratio should be considered for the analysis.

Species after Catalysis

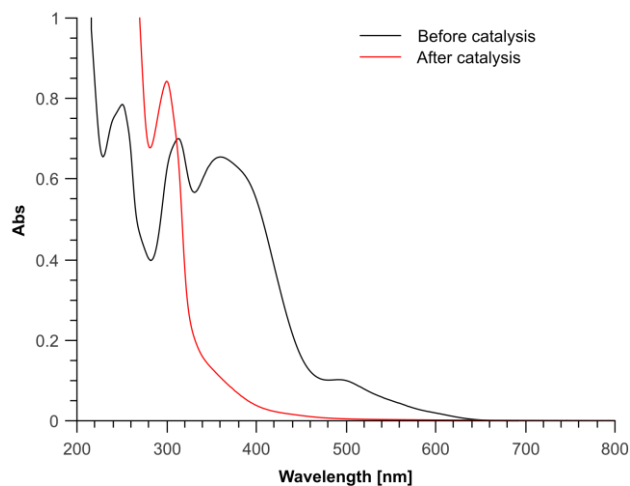


Figure S 29: UV-vis spectroscopy ($c = 2.51 \cdot 10^{-5} \text{ mol} \cdot \text{L}^{-1}$) before and after catalysis in aqueous triflic acid ($c = 0.1 \text{ mol} \cdot \text{L}^{-1}$, pH 1). Samples were taken from a catalysis experiment before the addition and one hour after the addition of 100 equivalents of Ce(IV) and diluted with aqueous triflic acid to the same concentration.

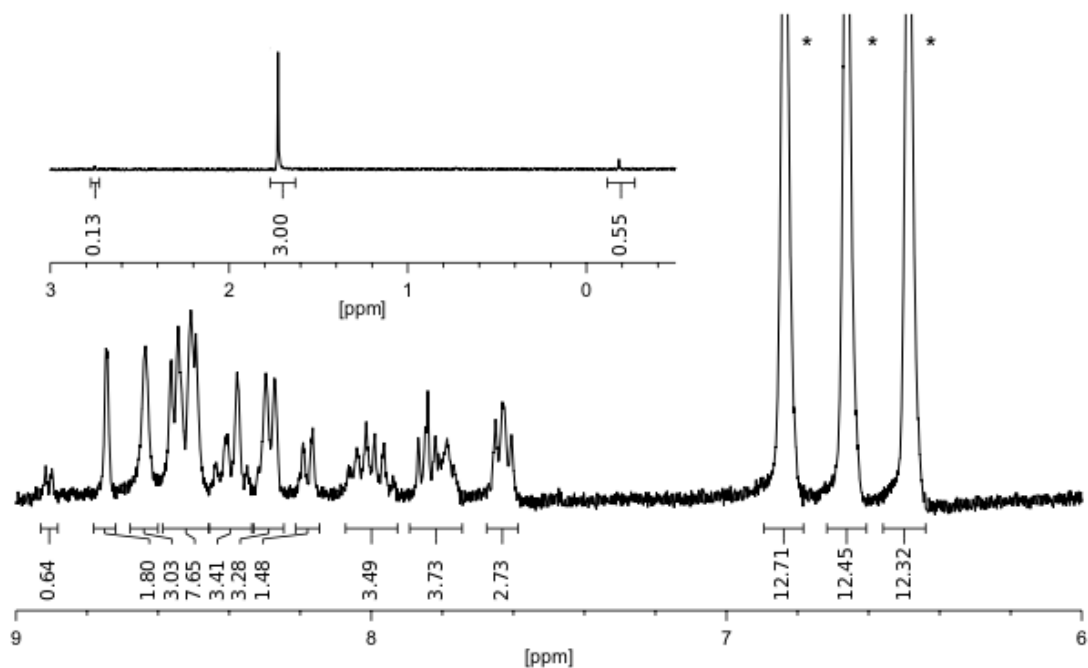


Figure S 30: ¹H-NMR spectrum (300 MHz) recorded 18 h after the addition of 100 equivalents of Ce(IV) to a sample of $\text{Na}\{1(\text{H}_2\text{O})_2\}$ in a solution of deuterio triflic acid in D_2O (approx. $c = 0.1 \text{ mol} \cdot \text{L}^{-1}$) at 303 K (*ammonium ions of CAN).

X-Ray Crystallography

empirical formula	C184 H160 F48 N40 O8 P8 Ru8
formula weight	5027.84
crystal size [mm ³]	0.45 × 0.16 × 0.12
crystal system	monoclinic
space group	<i>C2/c</i>
<i>a</i> [Å]	23.329(2)
<i>b</i> [Å]	18.055(3)
<i>c</i> [Å]	25.448(3)
α [°]	90.00
β [°]	114.892(8)
γ [°]	90.00
<i>V</i> [Å ³]	9723(2)
<i>Z</i>	2
$\rho_{\text{calcd.}}$ [g/cm ³]	1.717
<i>F</i> (000)	5024
μ [mm ⁻¹]	0.784
<i>T</i> _{min} / <i>T</i> _{max}	0.6098 / 0.8432
θ range [°]	1.48 - 26.84
<i>hkl</i> range	-29 - 29, -21 - 22, -32 - 32
measured refl.	49636
unique refl. [<i>R</i> _{int}]	10324 [0.0696]
observed refl. (<i>I</i> > 2 σ (<i>I</i>))	6972
data / restraints / param.	10324 / 134 / 688
goodness-of-fit (<i>F</i> ²)	0.853
<i>R</i> ₁ , <i>wR</i> ₂ (<i>I</i> > 2 σ (<i>I</i>))	0.0369, 0.0689
<i>R</i> ₁ , <i>wR</i> ₂ (all data)	0.0720, 0.0753
resid. el. dens. [e/Å ³]	-0.878 / 0.812

Table S3: Crystal data and refinement details of **2**(PF₆)₂

References

- [1] I. P. Evans, A. Spencer, G. Wilkinson, *J. Chem. Soc. Dalton Trans.* **1973**, 204–209.
- [2] B. Schneider, S. Demeshko, S. Neudeck, S. Dechert, F. Meyer, *Inorg. Chem.* **2013**, *52*, 13230.
- [3] M. Wojdyr, *J. Appl. Cryst.* **2010**, *43*, 1126-1128.
- [4] K.J.R. Rosman, P.D.P. Taylor *Pure Appl. Chem.* **1999**, *71*, 1593-1607.
- [5] G. M. Sheldrick, *Acta Crystallogr.* **2008**, *A64*, 112.
- [6] F. Bozoglian, S. Romain, M. Z. Ertem, T. K. Todorova, C. Sens, J. Mola, M. Rodriguez, I. Romero, J. Benet-Buchholz, X. Fontrodona, C. J. Cramer, L. Gagliardi, A. Llobet, *J. Am. Chem. Soc.* **2009**, *131*, 15176.